TOSCA 101191394
Manufacturing Processes and Digital **To**ols for more **S**ustainable **C**omposite **A**erostructures

Deliverable D5.1: "Intermediate demonstration and evaluation"

Due date of deliverable: 2026-06-30
Actual submission date: 2026-06-29

Start date of project: 1st January 2025 Duration: 36 months

Coordinator:
Christian Eitzinger, Profactor

Lead Beneficiary: FIDAMC
Contributions by: all Partners

Dissemination Level		
PU	Public	X
SEN	Sensitive information	

TOSCA Project is entirely funded by the European Union, under the topic HORIZON-CL5-2024-D5-01-08 of the Horizon Europe Framework Programme (HORIZON). Views and opinions expressed are however those of the author(s) only and do not necessarily reflect those of the European Union or the European Climate, Infrastructure and Environment Executive Agency. Neither the European Union nor the granting authority can be held responsible for them.

Funded by the European Union

History of Changes

Change made	Explanation
2026-06-29 First submission	
2026-08-04 Design change of the front page	EU logo and funding statement was missing
2026-08-04 Minor corrections to the text and to figure captions	As suggested by the Project Officer.

Contents

1. SUMMARY

This deliverable presents the intermediate demonstration and evaluation of the manufacturing, curing, joining, repair, structural health monitoring, digitalization, and recycling processes developed in the project. The demonstrations were performed experimentally at coupon level using representative structural features. The results confirm the feasibility and current maturity of the developed technologies relative to the project KPIs.

2. INTRODUCTION

2.1 Objectives

The objective of this deliverable is to document the intermediate demonstration and evaluation of the materials, processes and technologies developed within the project. This demonstration represents a key step toward validating the feasibility and industrial applicability of the vitrimeric-based composite system and associated manufacturing, monitoring, and lifecycle processes.

Specifically, this deliverable aims to:

- Demonstrate the manufacturability of vitrimeric-based CFRP composite materials at coupon level, including representative structural features relevant to future aeronautical applications.
- Experimentally validate the AFP lay-up process using the developed vitrimeric-based CFRP tapes, including the integration of quality monitoring systems and sensor technologies.
- Demonstrate and evaluate curing processes using different industrial manufacturing approaches and assess their compatibility with the developed materials and manufacturing workflows.
- Demonstrate the feasibility and performance of joining and repair processes adapted to vitrimeric-based composite materials.
- Demonstrate the integration and functionality of structural health monitoring (SHM) systems, including sensor embedding and data acquisition under representative conditions.
- Demonstrate the digitalization approach, including data acquisition, management, and integration into digital twin models for manufacturing monitoring and future predictive capabilities.
- Demonstrate the recyclability of the developed vitrimeric-based composite materials and validate the associated recycling processes at laboratory scale.
- Experimentally assess the maturity and readiness of the demonstrated processes relative to the project key performance indicators (KPIs), identifying strengths, limitations, and areas requiring further optimization.
- Provide documented experimental evidence of the demonstrations, including test results, observations, and demonstration records (photos, videos, and measured data).

This deliverable supports the transition from process development (WP3 and WP4) towards the manufacturing of integrated demonstrator parts and validation in the subsequent project phases.

2.2 Scope of the Deliverable

The deliverable documents the intermediate experimental demonstration and evaluation of the materials, manufacturing processes, monitoring technologies, digitalization capabilities, and recycling approaches developed within the project.

The scope of these deliverable focuses on the validation of individual processes at coupon level under representative manufacturing conditions. These demonstrations are intended to verify the technical feasibility, process compatibility, and current maturity of the developed solutions prior to the final demonstrator manufacturing. The integration of these processes into the final structural demonstrators will be addressed in subsequent project activities.
The results presented in this deliverable provide experimental evidence of the current maturity of the developed technologies and support their further development and validation in the next stages of the project.

2.3 Relation to Project Work Plan

This deliverable is part of Work Package 5 (WP5) and represents a key milestone in the validation of the processes and technologies developed throughout the project. It builds upon the developments performed in Work Packages 3 and 4 and provides experimental verification of their implementation under representative manufacturing conditions.
The materials demonstrated in this deliverable were developed in WP3, where CIDETEC formulated the vitrimeric-based resin systems and manufactured the corresponding prepreg tapes. In addition, WP3 included the development and optimization of curing, joining, repair, and recycling processes, involving CIDETEC, GMI, ÉIRE, AIMEN, and FIDAMC. The curing process parameters, joining methods, repair approaches, and recycling strategies defined in WP3 are experimentally validated and assessed in this deliverable.
Work Package 4 focused on the development and implementation of manufacturing processes, quality monitoring, and structural health monitoring technologies. In this context, FIDAMC and ADDCOMP implemented the AFP lay-up process using the developed materials, while Profactor developed and integrated quality monitoring sensors. GMI and ITA contributed to the development and integration of structural health monitoring systems and their associated data acquisition and interpretation methods. The experimental validation of these manufacturing and monitoring capabilities is documented in this deliverable.
This deliverable directly supports the objectives of WP5, which aims to perform intermediate demonstration and evaluation of the developed processes and technologies at coupon level. The demonstrations described herein assess the current maturity of the individual processes relative to the project Key Performance Indicators (KPIs) and verify their readiness for integration into full demonstrators in the subsequent phases of the project.
The results presented in this deliverable provide essential feedback to the project partners, enabling further refinement and optimization of the materials, processes, and monitoring systems prior to large-scale demonstrator manufacturing and final validation.

3. DEMONSTRATION OVERVIEW

3.1 Demonstration approach

The intermediate demonstration was carried out through experimental validation of the developed materials, manufacturing processes, monitoring systems, and recycling capabilities at coupon level. The demonstrations were performed using representative composite laminates manufactured with the vitrimeric-based systems developed in the project.

The demonstrations included manufacturing trials, curing operations, joining and repair activities, sensor integration, and data acquisition, allowing assessment of process performance, functionality, and readiness for subsequent demonstrator-level implementation.

3.2 Demonstrated Processes Overview

The following table summarizes the processes demonstrated in this deliverable and the partners involved in their experimental validation.

Process	**Partner**
Material manufacturing	CIDETEC
AFP lay-up & Quality control	FIDAMC, ADDCOMP, Profactor
Curing processes	CIDETEC, ÉIRE, FIDAMC
Joining Process	AIMEN, ÉIRE
Repair process	GMI, ÉIRE
SHM integration	ITA, GMI
Digitalization: data management & digital twin	ITA, Profactor, GMI
Recycling	CIDETEC, NOMA

Table 1: Processes Demonstrated in the Deliverable and Partners Involved in Experimental Validation

4. DEMONSTRATION RESULTS

4.1 Material manufacturing

This section aims to demonstrate the manufacturability and handling of the vitrimer-based prepreg tapes developed within the project. The work focuses on assessing their processability during automated composite manufacturing and evaluating their suitability for producing representative composite structures

4.1.1 Methodology

The methodology to demonstrate the manufacturability and handling of the vitrimeric-based prepreg tapes and to confirm their suitability for composite manufacturing processes is mostly based on the completion of the activities carried out in T3.1, reported in D3.1:

When formulating the vitrimer, referenced as **TS-1**, the fulfilment of the three related KPIs was verified:

- Storage conditions of the enduring tape: Stable at 17-25 °C (room temperature, RT).
- Enduring tapes processable by AFP at any curing degree.
- Glass transition temperature (Tg) of fully cured vitrimer: ≥170 °C

Also, other specifications associated with the production of the prepreg and tapes for AFP process in enduring stage, and the weldability, repairability and recyclability of the panels produced with them were studied and confirmed.

The production process of prepregs and subsequent production of tapes with TS-1 vitrimer were studied and optimized. Several iterations were required to optimize both the prepreg production process and their cutting into tapes. Then, prepreg and tapes were produced and supplied to other partners so they could move forward with their tasks in WP3, WP4 and WP5, especially in activities related to the production of panels by AFP, the main approach in the project.

4.1.2 Results

The vitrimer was formulated considering the three target KPIs, the requirements defined in WP2 for prepreg manufacturing, AFP process usage, and the weldability, repairability, and recyclability of the final composite component. To meet prepreg manufacturing needs and achieve a T_g above 170°C, a combination of epoxy resins with different viscosities were selected in Part A, including tetrafunctional and bifunctional monomers. The enduring stage of the material was achieved incorporating a dynamic hardener, 4-aminophenyl disulfide (4-AFD), as Part B, which provides a stable T_g during storage at room temperature. Furthermore, aerospace-grade vitrimer formulations, with their very high T_g, have a very narrow temperature window for activating their dynamic properties: the lower limit is just above the glass transition temperature (T_g), while the upper limit is constrained to 210 - 220 °C due to thermal degradation. To mitigate this limitation, the vitrimer dynamism was increased by incorporating an additional epoxy monomer with disulfide bonds into Part A. The resulting formulation was referenced as TS-1.

Once the TS-1 formulation was adjusted to meet the specified requirements for the cured vitrimer, it was characterized to verify its compliance with different sets of requirements. The results showed that the TS-1 formulation meets them not only for prepreg manufacturing but also for its use in the AFP process and for the final aeronautical application. In addition, stability, allowing long-term storage at room temperature, should facilitate handling and logistics.

State	Test	Value	Test method	Units	Requirements	TS-1 properties
Uncured	Isothermal viscosity by rheometer	Viscosity	-	Pa.s	1-10 (impregnation)	2-3 at 40°C
	T_g evolution by DSC @ RT and 50°C (accelerated)	T_g midpoint	EN6041	°C	Stable at RT (in enduring stage)	50-64 (≥14 months)
Enduring	Dynamic viscosity by rheometer	Viscosity min	EN6043	Pa.s	100 - 1.000 (AFP)	240 at 105°C
	Tackiness	Tack, Wt		$\mu J.mm^{-2}$	100 (AFP)	80-150 at 100ºC
Cured	T_g by DMA	T_g onset	EN6032	°C	> 170	171
	Dynamism by DMA	Relaxation time @ 200°C	-	s	-	25
	Dynamism by S-S bond content calculation	Disulfide bond content	-	S-S mol/g	$\geq 2.10^{-3}$	2.10^{-3}

Table 2: Summary of TS-1 characterization results versus initial requirements

The verification of the three target KPIs included:

- **Storage conditions of the enduring tape: Stable at 17-25 °C (room temperature, RT)**. By studying the evolution of T_g of the vitrimer over time at room temperature, a stabilization of T_g was observed in a range of 50 - 64 °C, corresponding to the enduring stage, for at least 14 months. Verification will continue over the coming months. A curing degree of 55% was measured in this range of T_g, which means that this is the maximum curing degree that the tape produced with TS-1 can reach when stored at room temperature.

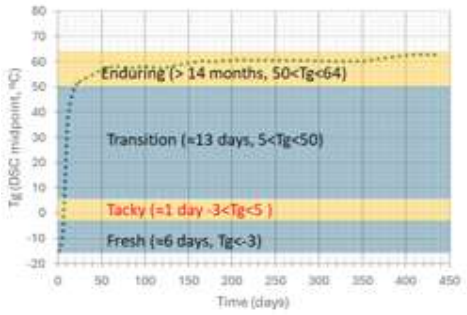

Figure 1: Evolution of T_g over time at room temperature for TS-1 vitrimer.

- **Enduring tapes processable by AFP at any curing degree.** Dynamic viscosity analysis showed that the vitrimer in enduring stage reaches the necessary viscosity for AFP when heated at 105°C. This partially demonstrated its processability by confirming that tapes with a curing degree of up to 55% can be placed automatically. The validation that the tapes can be consolidated and fully cured afterwards was studied in Task 3.2 and documented in this Deliverable, section 4.3.

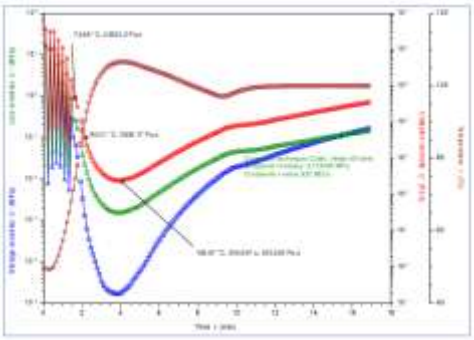

Figure 2: Viscosity profile of TS-1 in enduring stage when heating to 100°C at 30°C/min.

- **Glass Transition Temperature (T_g) of fully cured vitrimer: ≥170 °C**. A T_g onset of 171,3°C was obtained by DMA analysis of fully cured vitrimer.

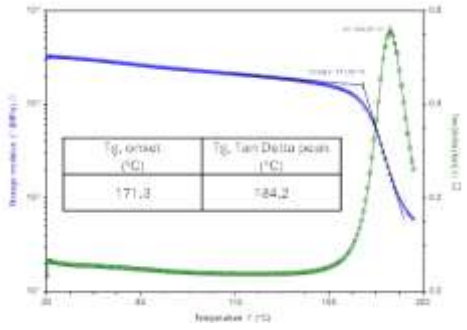

Figure 3: *T_g value of fully cured TS-1 vitrimer, measured by DMA at 5°C/min.*

Regarding the production of prepregs and tapes with the formulated vitrimer, A first study was conducted to define the production parameters for the enduring prepreg and its subsequent cutting into 0.5-inch tapes. After production of a first batch of prepreg and tapes, some areas for improvement were identified, such as the embossed films' texture on the tape surface and its fraying during cutting, which was very similar whether using slitting or saw-cutting methods. In the second study, the embossed films were replaced with smooth films, and the tapes were obtained by saw-cutting on the prepreg in its tacky stage instead of its enduring stage to eliminate fraying.

Figure 4: Tapes produced in the first batch

After the second batch provided satisfactory results, a third batch of tapes was produced under the same conditions for AFP process optimization by FIDAMC. Also, prepreg was produced to research its curing cycle and to provide AIMEN and EIRE with material to produce the first welding panels and reference panels, respectively.

The third batch showed several limitations not detected in previous batches. Specifically, it was noted that in many rolls the tape width was outside the acceptable range (below or above 0.5 inches), and that the maximum length of the rolls obtainable was 30 linear meters. Both limitations were associated with the saw-cutting method.

Figure 5: Details of dimensional defects of the tapes produced in the third batch.

Furthermore, FIDAMC reported difficulties in processing double-film tapes, as well as high stiffness and internal stresses that hinder and slow down the deposition process. The high stiffness is directly related to the enduring tape's solid state, while the internal stresses are attributed to the unwanted stretching of the smooth films during prepreg production.

Therefore, for future production runs in work packages WP6-WP8, it is proposed to replace the saw cutting method with a slitting method. This will allow for the removal of one of the two films, resulting in greater width tolerance and the possibility of obtaining longer rolls, either by cutting longer prepreg rolls or welding several tape rolls together. Additionally, silicone-coated paper will be used instead of the two smooth films to eliminate internal stresses in the tape. To reduce stiffness, it is proposed to slightly heat the tape after its unwinding and before guiding it to the deposition stage, as this has been observed to significantly reduce stiffness.

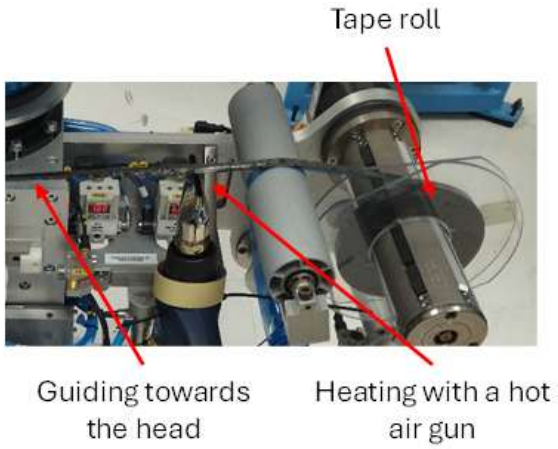

Figure 6: Heating of the tape after unrolling

Finally, in order to facilitate 3R welding, it is proposed to include on the surfaces to be welded a surface film of TS-1 vitrimer, which will have been previously integrated during the production process of the panels and will be produced in a similar way to the carbon fiber prepreg, replacing it with a low-grammage fiberglass veil.

4.2 AFP lay-up & Quality control demonstration

This section demonstrates the automated lay-up of the developed vitrimer-based composite tapes and validates the integration of quality monitoring technologies during manufacturing.

4.2.1 Methodology

The AFP lay-up and quality control demonstration was carried out at Addcomposites' facility in Espoo, Finland, and at FIDAMC's facility in Madrid, Spain. Addcomposites and Profactor focused on AFP head development, quality sensor integration, and high-feedrate placement characterisation at the Espoo facility. FIDAMC conducted the consortium panel manufacturing programme using the project material.

Addcomposites developed and supplied the AFP lay-up heads used in the demonstration. Two systems were deployed:

- **AFP-XS (single-tow, 1/2" channel width):** The AFP-XS compact head was modified for processing the CIDETEC vitrimer prepreg by adapting the tape channel to 1/2" width, matching the slit tape width supplied by CIDETEC. The AFP-XS was installed at FIDAMC and used for all consortium panel manufacturing.
- **AFP-X (4-tow, 4× 1/4" channels):** The AFP-X 4-tow head was used at the Addcomposites facility for quality monitoring integration and feedrate characterisation. Initial AFP-X trials were conducted with standard thermoset prepreg 1/4" tapes. The AFP-X head was upgraded to a 4× 1/2" channel configuration ahead of the M18 General Meeting to match the TOSCA vitrimer prepreg slit width. AFP placement at 1.2 m/s with the TOSCA vitrimer material has not yet been demonstrated; two limiting factors were identified: (1) the material in its as-received state requires pre-heating before tape entry to avoid fibre breakage due to its low flexibility; (2) reaching the 1.2 m/s target with the vitrimer material requires the flash lamp high-temperature heating system, integration of which is planned for Period 2.

FIDAMC panel manufacturing used CIDETEC TS-1 vitrimer prepreg in the enduring state, slit to 1/2" width. AFP-X integration and feed rate trials at Addcomposites used standard 1/4" thermoset prepreg, appropriate for validating the initial sensor integration, data pipeline, and speed capability independently of the specific surface and optical properties of the vitrimer material.

The full account of the FScanH sensor integration - including mechanical mounting, electrical and data connections, KUKA FSD (Fast Send Data) protocol installation on the AFP-X KRC4 controller, and digital trigger interface - is reported in Deliverable D4.2 (Lay-up Monitoring Sensor Integration). The present section summarises the integration outcome and reports the demonstration results.
Briefly, the FScanH sensor (Profactor) is mounted on the AFP-X structure to scan the freshly deposited layer during the robot's return stroke between passes. Robot pose data are streamed to the FScanH acquisition system in real time via the KUKA FSD protocol (UDP, 1 ms cycle), georeferencing each scan frame in the part coordinate system. AFP process data from AddPath and FScanH inspection data are recorded simultaneously to two separate HDF5 files, both conforming to the Dassault Systèmes Composite manufacturing database schema defined in Deliverable D4.4 and correlated post-run by ply number and timestamp.

The physical integration was completed during a joint session with Profactor's engineer Naveen Mula at Addcomposites' Espoo facility (31 March - 2 April 2026). Mechanical integration was led by Cagatay Akturk (Addcomposites); FSD protocol configuration and electrical setup by Khang Nguyen (Addcomposites). Standard quarter-inch reference prepreg was used during the April session to isolate sensor- and control-integration variables from material-specific variables and to preserve vitrimer material for the FIDAMC panel campaign.

The demonstration assessed: (1) end-to-end functionality of the FScanH inspection pipeline at AFP-X lay-up speeds, including ply-image stitching quality and georeferencing accuracy; and (2) maximum achievable deposition speed of the AFP-X head, targeting the project deposition speed objective of 1.2 m/s. Lay-up quality at increasing feedrates was monitored via the FScanH and the co-mounted thermal camera.

Quality control during lay-up will be achieved by use of the FScan sensor, which works based on the photometric stereo principle and mounted directly behind the lay-up head. Specifications and working principles of the sensor, as well as photometric stereo on which they are based on, have been presented in detail in deliverable D4.2. That deliverable also contains documentation of the initial integration tests, where the sensor was successfully mounted on the lay-up robot and first scans with the proposed scanning speed of 1.2 m/s were performed. Full performance of the inspection system, however, has not yet been achieved and will need to be demonstrated during a second testing run at Addcomposites facilities. These tests will include:

- Demonstration of starting and stopping of the scanning process at the correct points of the robot trajectory via signals from the KUKA robot.
- Demonstration of the ability to perform in-line scans of the lay-up of the project's vitrimeric prepreg tapes on a coupon level with a spatial resolution of 50 µm.
- Demonstration of the ability to segment and detect defects in the material (with detection margins outlined in D4.2) at a scanning speed of 1.2 m/s.

A second demonstration run was conducted at Addcomposites' Espoo facility following resolution of the interface issues identified in April. The run confirmed: start/stop signals from the KUKA controller were transmitted at the correct robot positions and reliably interpreted by the sensor; in-line FScanH scanning of the TOSCA TS-1 vitrimer prepreg was performed at 1.2 m/s with image quality sufficient for defect segmentation; AFP placement of the TOSCA vitrimer material at 1.2 m/s in combination with quality control scanning will be demonstrated once the flash lamp heating integration is complete.

AFP panel production was carried out at FIDAMC, using the developed TS-1 vitrimer-based prepreg tapes. The work was be performed in close collaboration between FIDAMC and Addcomposites and was built upon

the process optimisation activities previously reported in Deliverable 4.1, where the influence of deposition temperature, lay-up speed, compaction pressure, and feeding configuration on the manufacturability of the material was evaluated.
The methodology focused on demonstrating stable and repeatable AFP deposition of vitrimer-based composite panels under the optimised processing conditions identified during the previous trials. Particular attention was be given to the specific challenges associated with the material system, including delayed tack activation, tow width variability, internal fibre tension, limited flexibility, and the management of the dual release film configuration required by the prepreg format.
Based on the optimisation work described in D4.1, the AFP process was performed using a processing temperature of approximately 100°C to ensure sufficient resin mobility and inter-tow adhesion. Due to the delayed activation kinetics and relatively high viscosity of the vitrimer resin system, reduced lay-up speeds **(0.1 m/s**) was be employed to guarantee stable bonding conditions and minimise defect formation. Similarly, the selected compaction force **(0.5 MPa**) was identified as the best compromise between tow stability, geometric consistency, and adhesion quality during the optimisation trials.
The demonstrations performed at FIDAMC specifically focused on validating the manufacturability of the vitrimer-based material and demonstrating the stable production of composite panels under the selected thermal and compaction conditions mentioned above. These activities will confirm the applicability of the optimised AFP processing window established during the previous development phase.
Although the processing conditions currently required for the vitrimer material impose deposition speeds below the project target KPI of 1.2 m/s, the trials provide a critical validation of the material-process compatibility and establish the operational process window for stable manufacturing.

4.2.2 Results

AFP-X Integration and Feedrate Demonstration

The FScanH integration was completed and fully validated during the April 2026 on-site sessions (detailed in D4.2, Section 5). The end-to-end system - sensor mounted, 5 Gbit/s data link live, FSD position stream verified at 1 ms cycle, digital trigger confirmed, and AddPath HDF5 process logging active - was exercised during live lay-up runs on the AFP-X. Stitched ply images assembled from successive FScanH frames showed coherent coverage with no missed zones or stitching discontinuities, confirming that georeferencing via the FSD TICK timestamps was accurate at the intended lay-up speed.
During the integration tests, a spooling problem where the tape continued to get tangled up was encountered. A temporary fix in the form of adhesive tapes was performed, after which stable lay-up was possible.
The AFP-X 4-tow head demonstrated lay-up at 1.2 m/s, however, with a non-vitrimeric thermoset tape, as the project's material was not available for the initial integration.

Figure 7: Initial integration of the sensor into the AFP-X lay-up head.

Four live lay-up sessions were conducted on 2 April 2026, with continuous HDF5 process data and FScanH inspection data recorded throughout.
As the automated start and stop signal communication between the robot controller and the sensor had not yet been fully implemented, the scanning procedure could not be performed as originally planned during the return stroke of the lay-up head. Instead, image acquisition was carried out in-line during the lay-up process itself. Despite this limitation, the image stitching process was successfully validated, and no missing scan areas were observed in the resulting datasets.
However, in the aftermath of the initial integration, a technical limitation of the camera system was encountered. Camera binning did not provide the originally expected reduction in frame readout time. On the contrary, the observed readout times increased when binning was enabled, which would theoretically

prevent flawless stitching at the target scanning speed of 1.2 m/s for the given spatial resolution and field of view. This may indicate a discrepancy between the previously reported lay-up speed and the actual process speed.

During the second scanning and lay-up demonstration, all previously encountered challenges during scanning were successfully overcome. As lay-up with the project-relevant material was not yet possible with the modified AFP-X head, a few tows were laid up manually, for which afterwards automated inspection has been demonstrated (figure 8).

Figure 8: Demonstration of the scanning process.

Furthermore, the communication interface between the robot controller and the sensor was fully implemented and validated. Start and stop signals were transmitted at the correct robot positions and interpreted reliably by the sensor system, enabling image acquisition exclusively during the return motion of the lay-up head, as originally intended.

In addition, a mechanical modification of the sensor assembly was implemented, increasing the working distance from 150 mm to 185 mm. This adjustment resulted in a change of spatial resolution from 27 µm to 34 µm and necessitated a repeat of the previously done calibration process (Figure 9).

Figure 9: Calibration after mechanical changes to the sensor

Although the resolution was slightly reduced, it remained significantly better than the project KPI target of 50 µm. Importantly, the reduced spatial resolution decreased the camera frame readout time sufficiently to enable stable operation at the target scanning speed of 1.2 m/s. The successful achievement of this performance can be observed in the scanning results presented in figure 10.

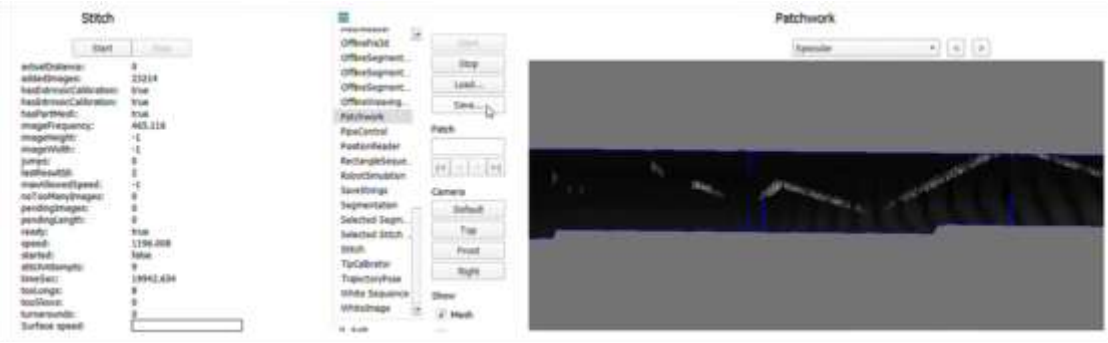

Figure 10: Scan results for a scanning speed of 1.2 m/s.

The combined KPI Status Dashboard for the lay-up inspection is presented on table 3.

KPI	Target	Status	Notes
Deposition Speed	1.2 m/s	**In Progress**	1.2 m/s demonstrated with standard reference prepreg (April 2026); AFP placement with TOSCA vitrimer prepreg requires flash lamp heating to maintain high temperature at high speed.
Material Throughput	Max achievable - current configuration	In progress	AFP-X 4× 1/2" mechanically ready; FScanH scanning at 1.2 m/s demonstrated with TOSCA vitrimer prepreg. AFP placement at 1.2 m/s with TOSCA material pending flash lamp integration.
Inspection Speed Compatibility	In-line with AFP at 1.2 m/s	**Demonstrated**	FScanH operational at 1.2 m/s after hardware changes.
Spatial Resolution	~50 µm	Demonstrated	Sensor calibrated and operational at a spatial resolution of 34 µm.

Table 3: KPI Status Overview for Lay-up inspection

The manufacturing of composite panels using the TS-1 vitrimer-based material was carried out by at FIDAMC facilities using the **AFP-XS head**, figure 11.

Figure 11: AFP-XS head at FIDAMC facilities

During the trials, the intrinsic characteristics of the TS-1 material significantly influenced its processability and required dedicated adaptation of both the processing parameters and the set-up configuration. In particular, the material behaviour in its enduring state differed from that of conventional tacky thermoset prepregs, requiring thermal activation before deposition in order to achieve sufficient tack, adhesion, and compaction.

Figure 12: AFP head configuration and feeding setup

One of the main challenges identified was related to the activation of tack during lay-up. The material required temperature activation, and the process temperature used during the trials was 100 °C. However, despite operating at this temperature, a delay was consistently observed between heating and the onset of effective adhesion. As a result, dwell times had to be introduced prior to deposition to ensure stable and repeatable bonding conditions. This behaviour is attributed to the relatively high viscosity and slower activation kinetics of the vitrimer system compared with conventional prepreg materials. In addition, during the lay-up process itself, even after thermal activation, the deposition speed had to be reduced to allow the compaction roller sufficient time to promote adhesion between layers. This was necessary to obtain acceptable adhesion and compaction quality in the final laminate. Based on the trials performed, the panels were manufactured using a deposition **speed of 0.1 m/s** and a **compaction setting of 0.5 MPa**. These conditions were

selected as a compromise between process stability, tape adhesion, and laminate quality.

A further constraint was associated with the presence of two release films in the prepreg/tape format. Unlike standard AFP materials, which typically include one or no release films, the TS-1 material required handling with two protective layers. This configuration was not directly compatible with the existing AFP head and feeding system and therefore required adaptations on the set-up. Several configurations were experimentally evaluated, including modifications to the feeding path, roller configuration, and release film management strategy. These adaptations were necessary to ensure proper tape guidance, avoid slippage, and enable stable deposition. Representative configurations and the associated challenges are presented in figure 12.
Additional deposition instabilities were also observed due to variability in the prepreg tow geometry and handling behaviour. The tows exhibited variations in width, internal tension, and limited flexibility, which affected their stability during feeding and placement. These factors contributed to local defects such as waviness, fibre misalignment, uneven deposition, and discontinuities in the laid material. Examples of these defects are shown in figure 13, where irregular fibre placement and local discontinuities can be observed. Cutting-related issues were also detected, leading to fibre breakage and irregular tow edges, further reducing deposition stability and increasing the occurrence of local defects.

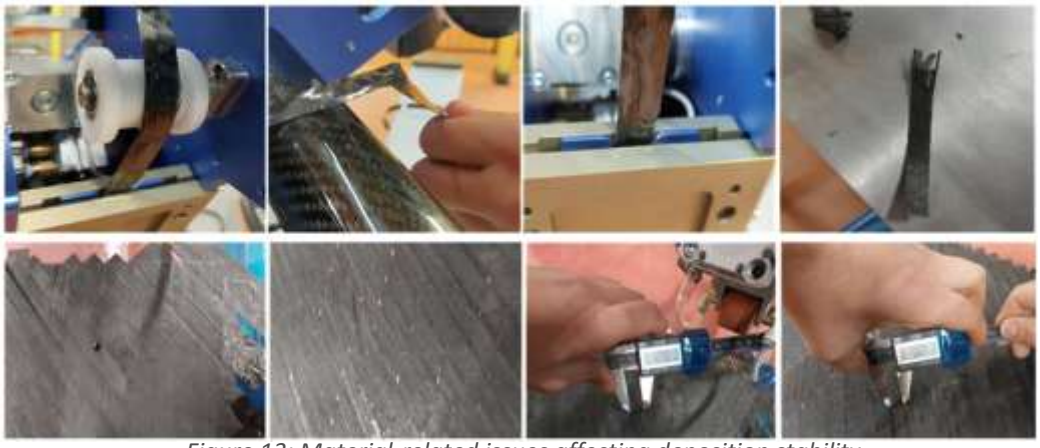

Figure 13: Material-related issues affecting deposition stability

It is important to highlight that, due to the nature of the TS-1 vitrimer-based material, thermal activation and sufficient contact time are expected to remain essential requirements when processing the material in its enduring state. In practice, the material cannot be assumed to behave like a conventional tacky thermoset prepreg during AFP lay-up. Instead, its manufacturing behaviour is closer to that of materials requiring heat-assisted deposition, such as thermoplastic-based systems, where temperature, pressure, and residence time play a critical role in achieving adequate bonding. For this reason, achieving deposition speeds in the range of 1.2 m/s, which are typically associated with standard tacky thermoset prepregs, would be technically challenging for this material without further optimisation. The use of such speeds should therefore not be directly assumed for the TS-1 system, since the material requires additional time under temperature and compaction to develop acceptable adhesion.

Some of the challenges identified during this manufacturing phase are expected to be addressed in the next phase of the project, as described by CIDETEC, the partner responsible for material development, in Section 4.1. Future material and process optimisation activities should therefore focus on improving tack activation, reducing the delay between heating and adhesion, improving tow dimensional stability and cutting quality.

Following the definition of the AFP configuration and processing parameters described above, the manufacturing of the TS-1 vitrimer-based composite panels was carried out at FIDAMC. The panel specifications were defined by each project partner according to the requirements of their respective

downstream activities, including defect generation, repair, structural health monitoring, welding, recycling, and additional validation tasks. FIDAMC was responsible for the fabrication of the panels using the adapted AFP process and the selected deposition conditions.

A total of **eleven panels** were manufactured with different dimensions, thicknesses, and lay-up requirements:

- One panel was produced for Profactor for defect-related activities, with dimensions of 600 × 400 mm and a thickness of 0.76 mm.
- For GMI, four panels were manufactured for repair activities, each with dimensions of 370 × 370 mm, a thickness of 3.0 mm, and a quasi-isotropic lay-up.
- In addition, one GMI panel was produced for structural health monitoring activities, with dimensions of 520 × 520 mm, a thickness of 2.0 mm, and a quasi-isotropic lay-up.
- The welding panel for AIMEN had dimensions of 500 × 500 mm, a thickness of 2.0 mm, and a quasi-isotropic lay-up.
- Two panels were produced for Eire Composites: one with dimensions of 620 × 440 mm and one with dimensions of 740 × 620 mm, both with a thickness of 2.5 mm and a quasi-isotropic lay-up.
- One panel was manufactured for CIDETEC recycling activities, with dimensions of 520 × 520 mm, a thickness of 2.0 mm, and a quasi-isotropic lay-up.
- One panel for Profactor for defect detection experiments with no specific lay-up orientation was defined.
- An additional panel was also produced for GMI Aero as part of the first trials involving TS-1 tapes with pre-embedded magnetoresistive sensors. The sensors were integrated into the tape prior to AFP processing. The objective of these preliminary trials was to evaluate the compatibility of the sensorised tapes with the AFP process, including tape feeding, guidance, heating, placement, and compaction. These trials provided initial feedback on the process adaptations that may be required to manufacture sensorised laminates using automated deposition.

Figure 14 show photographs of the panels.

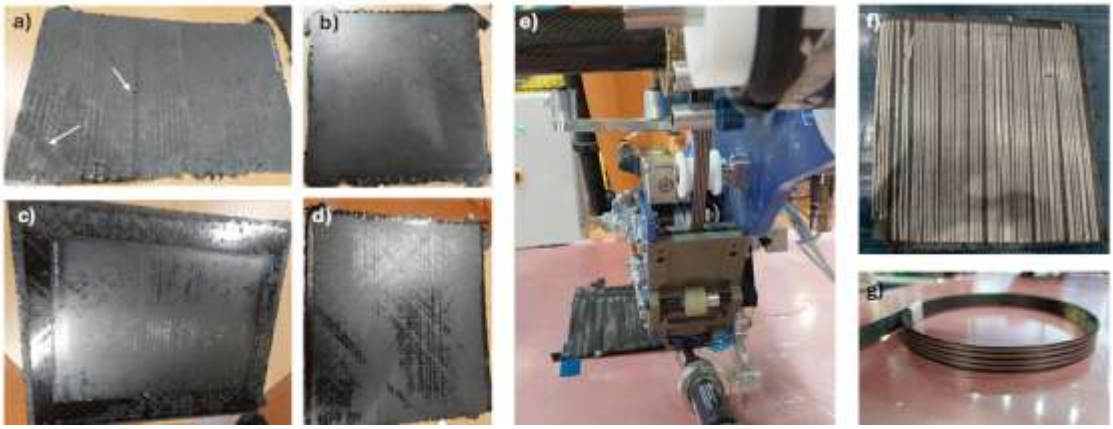

Figure 14: Overview of the manufactured panels and embedded sensor configurations:(a) panel with defects; (b) representative GMI repair panel with dimensions of 370 × 370 mm; (c) panels for EIRE; (d) representative 500 × 500 mm panels for CIDETEC, AIMEN, and GMI; (e) AFP lay-up representation for the tapes with sensors; (f) panel with sensors after curing; and (g) tape with embedded sensors.

Additional panels and specimens were also produced for ITA to support interlaminar fracture toughness testing (**figure 15**). These include unidirectional (UD) specimens for Double Cantilever Beam (DCB) and End-Notched Flexure (ENF) tests. The production included 20 UD specimens with dimensions of 250 × 25 mm and a thickness of 4.5 mm, and 20 UD specimens with the same in-plane dimensions and a thickness of 3.5 mm. In addition, 15 specimens measuring 200 × 200 mm were manufactured using a quasi-isotropic lay-up sequence for damage assessment and experimental testing.

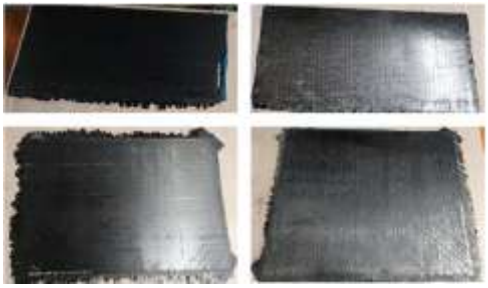

Figure 15: Panels manufactured for ITA

The KPI status dashboard for FIDAMC, focused on the AFP-XS head, is presented in Table 4

KPI	Target	Status	Notes
Deposition Speed	1.2 m/s	**In Progress**	The target deposition speed was not demonstrated due to the specific processing difficulties associated with the materials used. The 1.2 m/s target will require modifications to equipment and process parameters.
Panel production	Partner-defined panel number, dimensions, and configuration	**Demonstrated**	Panels were successfully produced according to the definitions and specifications provided by the partners.
Sensor layup	Demonstration of AFP lay-up using tapes with embedded sensors	**Demonstrated**	First trial of the lay-up of tapes with embedded sensors successfully demonstrated.

Table 4: KPI status for lay-up activities using the AFP-XS head.

4.3 Curing processes

This section demonstrates and validates curing processes for vitrimer-based composite materials using different industrial curing approaches

4.3.1 Methodology

CIDETEC defined the thermal curing cycle for prepreg and the tapes in T3.2, being reported in D3.2. The study served to complete the validation of the KPI corresponding to the processability of the enduring tapes after AFP process. Experimental data obtained during the study demonstrated the tapes processability. Moreover, feedback received from FIDAMC and ADDCOMP in their studies was be analysed to determine if the thermal curing cycle require any adjustments for future production runs.

FIDAMC demonstrated and validated the curing and consolidation processes of vitrimer-based composite panels manufactured through AFP lay-up using the TS-1 material system. The activities focused on evaluating different industrial curing approaches and assessing their influence on laminate quality, consolidation efficiency, and final thermo-mechanical performance.

Following AFP deposition, composite panels were consolidated using two alternative curing routes: hot-press consolidation and autoclave curing. Both routes were applied after AFP lay-up and were selected to

assess the effect of pressure level and consolidation conditions on the thermomechanical and mechanical performance of the laminates.

For the hot press route, the panels were placed between two plates and heated under controlled conditions. The cycle included gradual heating up to an intermediate temperature, where pressure was applied once sufficient resin flow was achieved, approximately at 90 °C. This was followed by a 60 min dwell stage to promote consolidation and air removal, and then by a final ramp to the curing temperature of approximately 180 °C, where the material was held to complete curing. The system was subsequently cooled under controlled conditions before pressure release. The maximum pressure applied during this process was 10 bar, providing direct compaction of the laminate.

In parallel, panels were also processed by autoclave curing using a comparable thermal cycle, but under different pressure conditions. In this case, consolidation was achieved through vacuum bagging combined with an autoclave pressure of approximately 30 psi, equivalent to 2.07 bar. Although this pressure was considerably lower than that applied in the hot press, it was combined with vacuum, in the range of 75 - 100 mmHg, to assist air removal and laminate consolidation. The effectiveness of both curing approaches was evaluated through a combination of microstructural, thermal, and mechanical characterisation techniques in order to assess consolidation quality, curing degree, and laminate performance.
The characterisation activities included:

- Optical microscopy analysis to evaluate laminate quality, thickness distribution, void content, and defect occurrence.
- Differential Scanning Calorimetry (DSC) to assess curing degree, residual reactivity of the vitrimer matrix and glass transition temperature (T_g).
- Dynamic Mechanical Analysis (DMA) to evaluate thermo-mechanical behaviour and glass transition temperature (T_g).
- Mechanical testing of ±45° laminates to assess the in-plane shear behaviour of the material.
- Interlaminar Shear Strength (ILSS) testing to evaluate interlaminar bonding quality and consolidation efficiency achieved under the different curing conditions.

4.3.2 Results

The thermal cycle to consolidate the tape or prepreg stacks from enduring stage (50°C<T_g<64°C) to fully cured stage (Tg>170°C) was studied and defined. A first plateau was defined at 90°C for 60 minutes, after applying a relatively fast heating speed (10°C/min) to achieve the minimum viscosity of the vitrimer as quickly as possible without additional curing, which would cause an undesired viscosity increase. The second plateau was defined at 180°C for 30 minutes to complete the curing of the vitrimer. When replicating the cycle in the rheometer, it was observed that the minimum viscosity reached was around 1200 Pa.s. Although this value was high, the established cycle was considered the best possible, as it would not be possible to reduce the viscosity under 1200 Pa.s with realistic heating rates due to the rapid viscosity increase in this curing phase. A good compaction of enduring tape during the AFP process would ensure a good consolidation using this

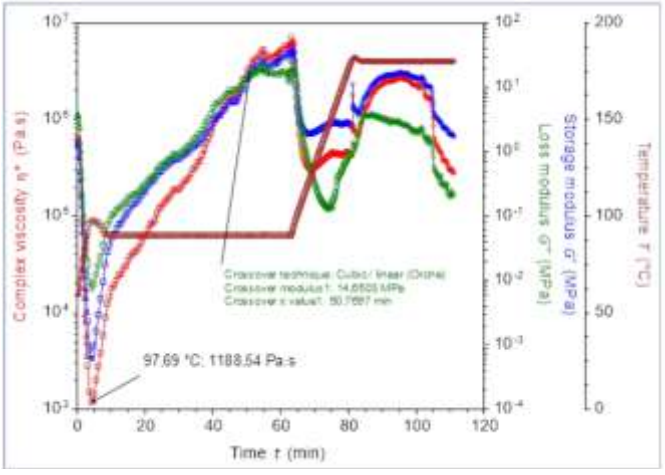

Figure 16: Viscosity profile for TS-1 formulation in enduring stage in rheometer

thermal cycle in oven or autoclave. On the contrary, a poor compaction during the AFP process would require applying higher pressure during the consolidation phase to compensate the reduced flow of the vitrimer, requiring a press instead of an oven or autoclave.

The study completed the verification that the tapes in enduring stage produced with TS-1 vitrimer can be consolidated until it is fully cured.

The curing processes assessed in this work builds directly on the process definition and validation activities reported in Deliverable D3.2, in which thermal cycles for the TS 1 vitrimer system were established for both tacky and enduring material states. The results presented in D3.2 demonstrated that the defined cure cycles consistently achieve full cure across the investigated processing routes, as verified by glass transition temperature measurements. On this basis, the present work does not seek to further optimise curing temperature profiles, but rather to evaluate the implementation of these curing strategies under representative manufacturing conditions aligned with the project objectives. **Figure 13** shows the macrophotos of the panels cured using oven and using autoclave.

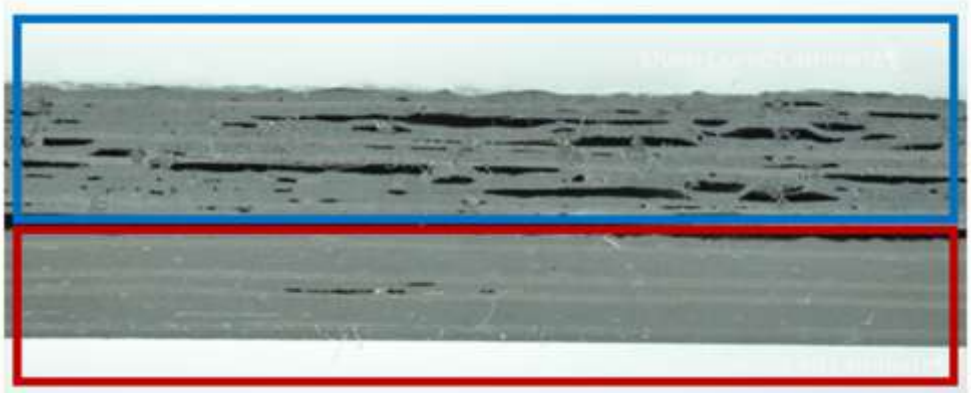

Figure 17: Macrophoto comparison between oven (top) and autoclave (bototom) laminates

In accordance with the TOSCA goals, particular emphasis is placed on the development and assessment of out of autoclave (OOA) manufacturing routes. Within this context, oven-based curing under vacuum-only conditions was selected as the primary processing route for evaluation, with autoclave curing employed solely as a benchmark to assess the level of laminate quality achievable under higher consolidation pressures. The objective of this section is therefore to determine whether the curing strategies defined in D3.2 can be effectively applied under OOA conditions to produce laminates of sufficient quality for subsequent processing and testing.

Initial panels cured under vacuum-only oven conditions exhibited significant limitations in laminate consolidation. Macro-scale inspection revealed widespread through-thickness porosity, incomplete contact between plies, and localised variations in laminate thickness. These observations are consistent with the material behaviour described in D3.2, where the vitrimer system exhibits relatively high viscosity during the

Figure 18: Macrophoto of laminate cured using resin dam. See bulging material and large internal voids.

consolidation phase, limiting resin flow and increasing reliance on externally applied pressure to achieve adequate fibre wetting and void removal.
In addition to porosity-related defects, the initial oven-cured panels also exhibited pronounced resin redistribution during processing. Excessive resin bleed was observed at the vacuum bag interface, while the tool-side of the laminate appeared comparatively dry, indicating non-uniform resin distribution through the laminate thickness. To investigate whether this behaviour could be mitigated, a trial incorporating a resin dam was conducted in an attempt to retain resin within the laminate during curing. The inclusion of the resin dam resulted in an improvement in the surface condition on the tool-side of the panel, indicating that resin retention at the interface was enhanced. However, this modification also led to non-uniform thickness distribution, characterised by localised material accumulation and bulging within the laminate (**Figure 18**). Furthermore, despite the improvement in surface finish, no corresponding improvement in through-thickness consolidation was observed, with significant porosity and incomplete ply contact still evident. These observations indicate that while resin flow can be influenced through local tooling modifications, control of resin bleed alone is insufficient to achieve effective laminate consolidation under vacuum-only conditions.

To further investigate whether consolidation could be improved through enhanced pressure distribution, a final oven curing trial was performed incorporating the use of a caul plate during lay-up. This trial, corresponding to panel EC RD 4143, was designed to distribute the applied vacuum pressure more uniformly across the laminate surface and reduce local pressure gradients introduced by the bagging configuration. The introduction of the caul plate resulted in improved surface finish and eliminated macroscopic bowing of the panel, indicating that the modification was effective in improving geometric stability during processing. However, macrophoto examination of the laminate cross-section confirmed that a high level of porosity persisted throughout the laminate thickness, with no significant improvement in ply consolidation observed relative to previous vacuum-only trials. Representative cross-sectional macrophoto (**Figure 19**) clearly demonstrate the presence of distributed voids and incomplete interlaminar contact within the laminate, despite the introduction of this tooling modification.

Figure 19: Macrophoto of laminate cured OOA using caul plate

In addition to the oven-based trials, ultrasonic inspection was performed on AFP-manufactured panels cured under elevated pressure conditions (11 bar) to assess laminate quality at panel scale. Representative C-scan results (**Figure 20**) show significant spatial variation in signal response across the panel, with no clearly defined uniform regions. The presence of widespread signal variation and localised indications suggests non-uniform internal laminate quality despite the application of high consolidation pressure.

These observations indicate that, in addition to curing conditions, variability introduced during earlier manufacturing stages, such as AFP lay-up, may contribute to the overall material condition. This variability

is carried through the curing process and results in non-uniform laminate properties at panel scale, which has implications for downstream operations where consistent material behaviour is required.

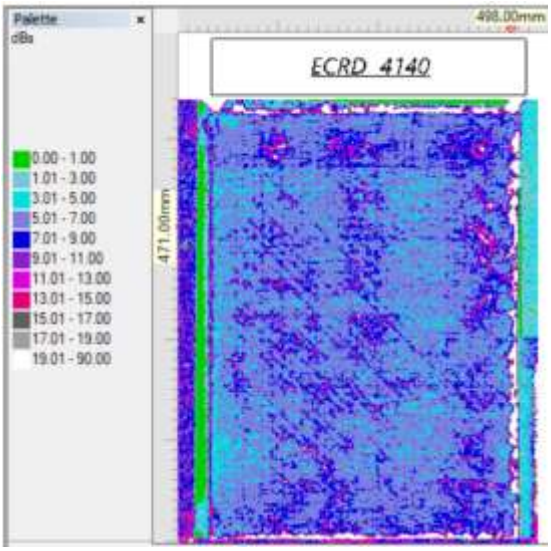

Figure 20: Ultrasonic C-scan of AFP-manufactured panel (EC-RD-4140) cured at 11 bar, showing significant variation in signal response across the laminate, indicating non-uniform internal quality

For comparison, panels cured under autoclave conditions exhibited a markedly improved level of consolidation, characterised by reduced void content, more uniform fibre distribution, and improved interlaminar integrity. This contrast highlights the critical role of applied pressure in achieving effective consolidation for the material system under investigation. While the curing cycles themselves are consistent across both processing routes, the difference in achievable consolidation pressure has a dominant influence on the resulting laminate quality.

Taken together, the results presented in this section demonstrate that the primary limitation of the oven-based OOA curing route is not associated with the thermal cycle or completeness of cure, but rather with the magnitude of the available compaction pressure during processing. The TS 1 vitrimer system exhibits limited flow during the later stages of cure and therefore requires sufficient external pressure to ensure adequate fibre bed compaction and void removal. Under vacuum-only conditions, the available pressure is insufficient to facilitate these mechanisms to the extent required for consistent laminate quality. As a result, defects introduced during lay-up are not effectively resolved during curing, leading to persistent porosity and reduced structural integrity.

From an assessment perspective, the curing strategy defined in D3.2 is technically robust from a thermal standpoint; however, its implementation under OOA vacuum-only conditions has not yet demonstrated the ability to achieve consistent laminate consolidation. While localised process modifications, such as resin dams or caul plates, can influence resin distribution and improve external panel characteristics, they do not address the underlying limitation associated with insufficient consolidation pressure.

The results obtained in this study indicate that vacuum-only OOA curing, in its current form, leads to persistent porosity and non-uniform laminate consolidation, primarily due to the limited compaction pressure available during processing. While increased consolidation pressure has been shown to improve laminate quality, the variability observed in AFP-manufactured panels indicates that consistent and uniform material properties are not yet fully achieved under current processing conditions. As such, further development of the OOA route remains feasible, with future work required to explore approaches to improving consolidation, including process modifications aimed at improving resin flow and fibre bed compaction, and potential material-level optimisation such as resin formulation adjustments to better accommodate reduced-pressure processing conditions.

The vitrimer-based composite panels manufactured by AFP lay-up were cured using two different industrial processing routes: hot press consolidation and autoclave curing. The objective was to compare the effect of each curing route on the final laminate quality and performance, considering differences in pressure application, consolidation conditions, and defect sensitivity.

Optical microscopy was used to evaluate the internal laminate morphology of panels cured by both methods (**figure 21**). In both cases, a similar amount of voids was observed, mainly elongated and aligned

with the fibre direction. Some regions highlighted in the microscopy images (blues circles) can also be associated with the stitching or binding yarns present in the CF UD slit-tape material. These features are related to the original tape architecture and should not be interpreted as curing-induced defects. The hot-press-cured panels showed a flatter surface and a more uniform laminate profile, which is likely related to the higher compaction pressure applied during processing. In contrast, the autoclave-cured panels presented more visible surface waviness and local fibre waviness around defect regions.

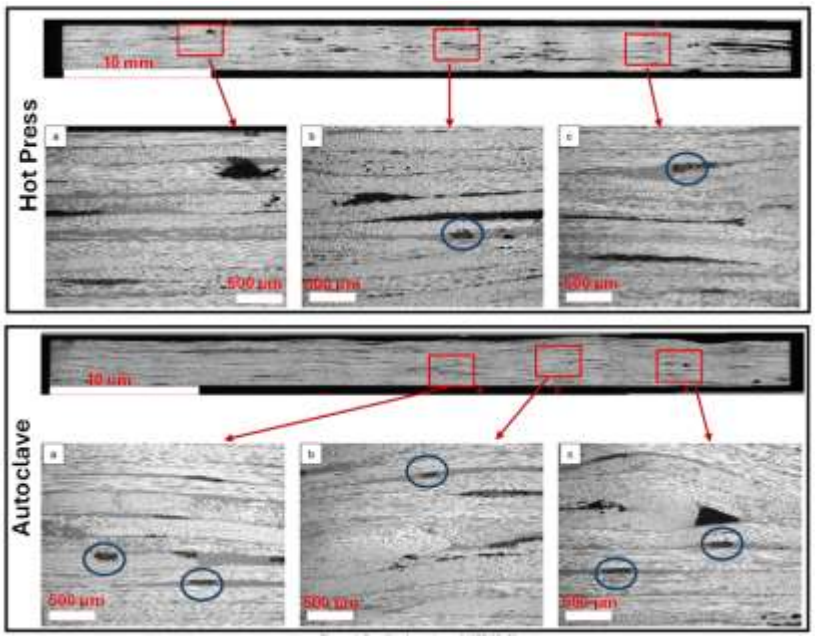

Figure 22: Optical microscopy images of vitrimer-based composite panels cured by hot press consolidation and autoclave curing

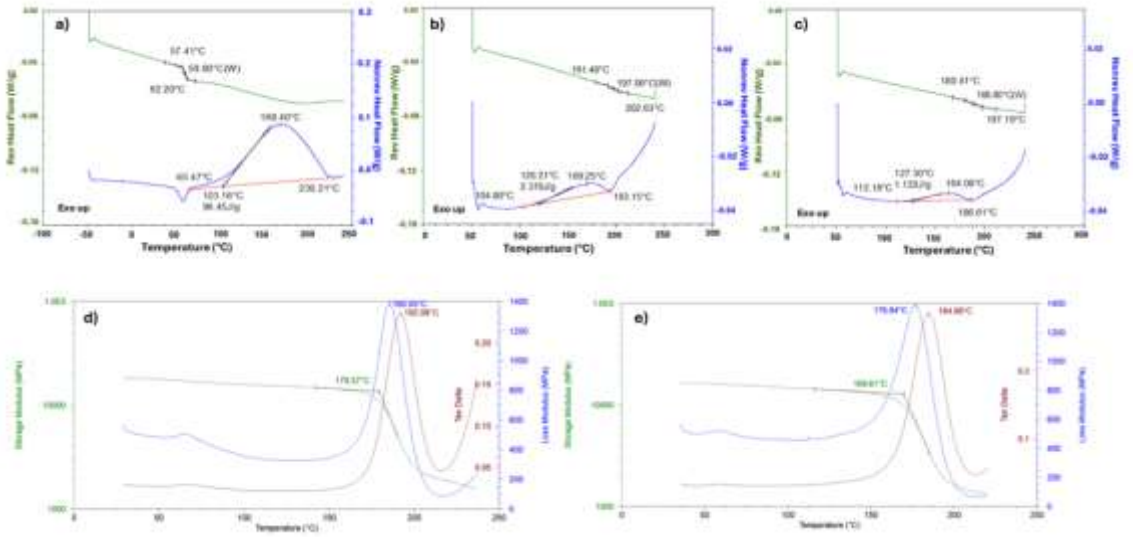

Figure 21: Representative DSC and DMA results: (a) DSC uncured vitrimer-based material; (b) DSC hot-press-cured laminate; (c) DSC autoclave-cured laminate; (d) DMA of hot-press-cured laminate; and (e) DMA of autoclave-cured laminate.

Figure 22 presents representative DSC and DMA results for the vitrimer-based material and the cured laminates. The DSC curves compare the uncured material with laminates processed by hot press and

autoclave curing. The DMA results complement this analysis by showing the thermomechanical behaviour of the hot-press- and autoclave-cured laminates.
The DSC and DMA results, summarized on **table 5**, show that both curing routes led to a high degree of cure, with values above 97%, confirming the suitability of both hot press and autoclave processing for curing the vitrimer-based laminates. The autoclave-cured panels showed a slightly higher degree of cure, 98.5 ± 0.3%, compared with 97.4 ± 0.1% for the hot-press-cured panels. However, the hot-press-cured laminates presented higher glass transition temperatures. The DSC T_g increased from 188.5 ± 0.3 °C for the autoclave route to 196.0 ± 1.1 °C for the hot press route. The same trend was observed by DMA, with higher T_g onset and T_g values (tan δ peak) for the hot-press-cured laminates. The DMA T_g onset increased from 169.9 ± 0.4 °C for the autoclave route to 178.1 ± 0.9 °C for the hot press route, while the DMA T_g (tan δ peak) increased from 184.7 ± 0.3 °C to 191.6 ± 0.4 °C.

Although the autoclave route resulted in a slightly higher degree of cure, the hot press route provided higher thermal and thermomechanical transition temperatures. This may be associated with the higher compaction pressure applied during hot pressing, which can promote better consolidation and a more uniform laminate structure. This interpretation is consistent with the microscopy observations, where the hot-press-cured panels showed a flatter surface and a more uniform laminate profile. In contrast, the autoclave-cured panels presented more visible surface waviness and local fibre waviness around defect regions. Overall, both curing routes were effective, but the hot press process resulted in a more uniform laminate morphology and higher transition temperatures.

Curing route	DSC T_g (°C)	Degree of cure, α (%)	DMA $T_{g\text{ - onset}}$ (°C)	DMA T_g, tan δ peak (°C)
Hot press	196.0 ± 1.1	97.4 ± 0.1	178.1 ± 0.9	191.6 ± 0.4
Autoclave	188.5 ± 0.3	98.5 ± 0.3	169.9 ± 0.4	184.7 ± 0.3

Table 5: Summary of DSC and DMA results for vitrimer-based laminates cured by hot press and autoclave processing.

Figure 23 presents the ILSS and IPSS results for the vitrimer-based laminates cured by hot press and autoclave processing. The corresponding values are summarized in **Table 6**.

The ILSS results show a clear difference between the two curing routes. The hot-press-cured laminates reached a maximum apparent interlaminar shear stress of 63.1 ± 2.0 MPa, compared with 44.4 ± 1.5 MPa for the autoclave-cured laminates. This indicates better interlaminar performance for the hot press route, which may be associated with the higher compaction pressure applied during curing. This interpretation is consistent with the optical microscopy observations, where the hot-press-cured panels showed a flatter surface and a more uniform laminate profile, while the autoclave-cured panels presented more visible surface waviness and local fibre waviness around defect regions.

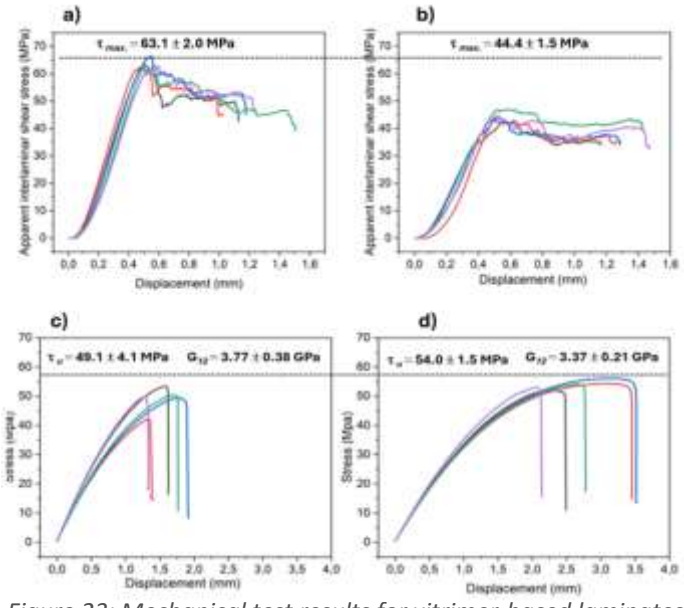

Figure 23: Mechanical test results for vitrimer-based laminates: (a) ILSS, hot press; (b) ILSS, autoclave; (c) IPSS, hot press; and (d) IPSS, autoclave.

For the IPSS results, the differences between both curing routes are less conclusive. The autoclave-

cured laminates showed a slight tendency toward higher ultimate in-plane shear strength, 54.0 ± 1.5 MPa, compared with 49.1 ± 4.1 MPa for the hot-press-cured laminates. However, considering the experimental scatter, this difference cannot be considered significant. Similarly, the in-plane shear modulus showed a slight tendency to be higher for the hot-press-cured laminates, 3.77 ± 0.38 GPa, compared with 3.37 ± 0.21 GPa for the autoclave-cured laminates, but the overlap between the error ranges prevents a clear distinction between both routes.

Test	Parameter	Hot press	Autoclave
Interlaminar Shear Strength (ILSS)	Maximum apparent interlaminar shear stress, τ_{max} (MPa)	63.1 ± 2.0	44.4 ± 1.5
In-Plane Shear Strength (IPSS)	Ultimate in-plane shear stress, τ_u (MPa)	49.1 ± 4.1	54.0 ± 1.5
In-Plane Shear Strength (IPSS)	In-plane shear modulus, G_{12} (GPa)	3.77 ± 0.38	3.37 ± 0.21

Table 6: Summary of ILSS and IPSS results for vitrimer-based laminates cured by hot press and autoclave processing

These mechanical results are consistent with the thermal, thermomechanical, and microscopy observations. Both curing routes achieved a high degree of cure, above 97%, confirming effective curing of the vitrimer-based laminates. Although the autoclave route showed a slightly higher degree of cure, the hot-press-cured laminates presented higher DSC and DMA Tg values, suggesting a stiffer and more thermally stable network response. Together with the microscopy observations, this supports the conclusion that the hot press route promoted better consolidation and interlaminar quality, which is mainly reflected in the improved ILSS performance. In contrast, the IPSS response appears to be less sensitive to the curing route, with only minor trends observed within the experimental uncertainty.

4.4 Joining Process

This section demonstrates the feasibility of joining processes compatible with vitrimer-based thermoset composite materials, assessing their applicability for recyclable composite structures.

4.4.1 Methodology

The joining methodology was defined to generate coupon-level experimental evidence on the feasibility of joining vitrimer-based composite laminates, with a primary focus on induction welding under representative processing conditions. The work was designed as an exploratory experimental campaign aimed at assessing the ability of the process to generate a stable bonded interface, while identifying key process limitations associated with the material system and available equipment.

Induction welding was selected as the primary joining route, based on its potential compatibility with vitrimer-based thermoset composites and its relevance for fast and scalable joining applications. The trials were performed using previously cured laminates, representative of components produced via the manufacturing routes established earlier in the project. Both autoclave-cured and oven-cured panels were used as substrates to assess the influence of laminate condition on joining behaviour.

The experimental campaign focused on assessing the influence of key process parameters, including applied power, heating time (dwell), and consolidation pressure, within the constraints of the available equipment. Processing conditions were selected in accordance with the thermal activation requirements of the vitrimer system, targeting a surface temperature of approximately 180 °C to enable bond formation through activation of the dynamic network. The available induction welding equipment imposed a maximum consolidation pressure of approximately 3 bar, and this constraint was maintained throughout the trials.

Attention was given to the ability of the induction system to generate sufficiently uniform temperature distribution across the bond interface, as this is a critical requirement for activation of the vitrimer network. The trials were therefore conducted in a controlled and exploratory manner, with emphasis placed on evaluating the combined effects of temperature distribution and pressure on the development of a continuous bonded interface.

Given the exploratory nature of the campaign, process optimisation was not the primary objective; instead, the work aimed to define the feasible processing window and identify any constraints preventing the formation of a continuous bond. Evaluation of the joined interfaces was performed at coupon level through visual inspection, handling assessment, and qualitative evaluation of bond continuity. Progression to mechanical testing, including Single Lap Shear (SLS), was defined as conditional upon the formation of joints demonstrating sufficient continuity and integrity under manual handling to justify specimen preparation and test execution. Within the scope of this deliverable, the methodology is therefore focused on feasibility assessment rather than full mechanical characterisation or process qualification. Where induction welding does not produce sufficiently robust joints, alternative joining approaches have been identified and are planned for investigation in subsequent work packages (WP6), including adhesive bonding methods.

The methodology to demonstrate the resistance welding capabilities and performance of carbon fibre reinforced composite with 3R vitrimer resin (TS-1 material system) is based on the extension of the mechanical characterization activities carried out in WP3 during the welding optimisation phase. In particular, once the optimal combination of material curing state and processing parameters has been identified - i.e. the conditions that maximise the mechanical performance as assessed through SLS lap shear tests - a more comprehensive mechanical characterisation campaign will be conducted.
This extended characterisation includes interlaminar shear strength (ILSS) tests using the short beam method, as well as Mode I and Mode II fracture toughness tests to evaluate the resistance of the welded interfaces under different loading and failure conditions. These tests provide a broader understanding of the joint performance beyond in-plane shear behaviour, allowing for a more complete assessment of structural integrity and damage resistance.
In addition, microstructural analysis was performed on selected welded specimens. The aim is to identify potential defects such as porosity, resin-rich areas, or localised lack of fusion at the welding interface. The combined mechanical and microstructural assessment enable correlation between processing conditions, interface quality, and resulting structural performance, thereby validating the robustness and repeatability of the proposed welding approach.

4.4.2 Results

The joining approach investigated in this work focused on induction welding of vitrimer-based composite laminates, with the objective of developing a rapid and scalable joining method compatible with the material system and processing routes established in earlier work packages. The trials conducted in this section represent an initial assessment of the feasibility of induction welding under the constraints of the available equipment and material configuration.

Induction welding trials were performed using a target processing surface temperature of 180°C, with an applied pressure of approximately 3 bar and a dwell time of 30 minutes. These parameters were selected to align with the thermal conditions identified in Deliverable D3.2 as being suitable for activation of the vitrimer network at the bond surface, while remaining within the operational limits of the available induction welding system. To date, trials have been conducted using both autoclave-cured and oven-cured panels, with the aim of evaluating the ability of the process to generate a consistent bond at the interface between laminates.

Across all trials performed, the induction welding process did not result in the formation of bonds of sufficient quality to justify mechanical testing. In all cases, any adhesion achieved at the interface was limited and highly localised, with bonded regions typically confined to small areas corresponding to zones of elevated temperature (**figure 24**). These bonds were not mechanically robust and could be separated under light manual loading, indicating that a stable and continuous joint was not formed.

Figure 24: Localised heating achieved through induction welding.

A key challenge observed during the trials was the non-uniform distribution of temperature across the intended bond interface. The heating generated by the induction system was concentrated in highly localised regions, resulting in a narrow processing window in which sufficient temperature could be achieved to activate the vitrimer behaviour without causing material degradation. As a consequence, regions of localised overheating were observed, particularly at the edges of the heating zone, while adjacent areas remained insufficiently heated to promote effective bonding. Surface evidence of thermal degradation was observed (**figure 25**) in these overheated regions, suggesting that the bonding that did occur was associated with resin softening or degradation rather than controlled vitrimer network rearrangement.

Figure 25: Thermal degradation of laminate at the edge of the panel causing light bond

In addition to thermal non-uniformity, the limited compaction pressure achievable with the available induction welding system was identified as a critical constraint. The maximum pressure of approximately 3 bar is significantly lower than that applied during autoclave processing and was not sufficient to ensure consistent intimate contact between adherends at the bond interface. As a result, even in regions where adequate temperature was locally achieved, the lack of sufficient pressure hindered the development of a continuous bonded interface, contributing to the observed weak and discontinuous adhesion.

The combined effects of non-uniform heating and insufficient consolidation pressure resulted in a highly constrained processing window, within which the simultaneous achievement of adequate temperature, pressure, and interfacial contact was not possible using the current setup. Furthermore, due to the absence of a stable bond, process development has to date been limited to stationary point welding rather than continuous or travelling weld configurations, preventing further evaluation of process scalability or repeatability.

It should be noted that the induction welding trials completed to date have been performed using panels manufactured via autoclave and oven curing. At the time of writing, additional trials using AFP-manufactured panels are planned, in order to assess the influence of laminate architecture and surface condition on the welding process. While no significant improvement in bonding performance is anticipated

based on the current understanding of the process limitations, these trials will provide further confirmation of the robustness of the observed trends across different panel types.

From an assessment perspective, the results obtained indicate that induction welding, as implemented using the current equipment configuration, is not yet capable of producing a consistent or mechanically viable bond for the vitrimer composite system. The primary limitations are associated with the restricted compaction pressure, limited to approximately 3 bar, and the inability to achieve uniform heating across the bond interface. These constraints result in a process that is dominated by localised and uncontrolled bonding phenomena rather than uniform activation of the vitrimer network.

It is noted that these limitations arise primarily from the capabilities of the available induction welding system, rather than from a lack of definition in the processing parameters. Within the scope of the current work, no viable process window has been identified under these constraints that enables consistent bond formation. Additional trials using AFP-manufactured panels are planned to confirm the observed behaviour across different laminate configurations; however, based on the results obtained to date, no significant improvement in bonding performance is anticipated.

As such, induction welding under the current processing conditions is not considered a viable joining route for the material system within the scope of this study. Alternative joining approaches will therefore be investigated in subsequent work packages, including adhesive bonding methods to be developed within WP6.

The results obtained during the experimental campaign carried out within WP3 and reported in Deliverable D3.3 showed that the highest welded-joint quality, in terms of lap shear strength as assessed by Single Lap Shear (SLS) testing, was achieved when joining laminates in the Enduring stage using heating elements also in the Enduring stage. The optimum welding condition was obtained by applying a current intensity of 18 A for 60 s, under a consolidation pressure of 6 bar. It is worth noting that, due to the larger specimen dimensions required for the determination of the welded joint fracture toughness (170 mm in length) compared to those used for the other mechanical tests (120 mm), the welds produced for fracture toughness characterization were manufactured using a consolidation pressure of 4 bar. Following welding, all specimens were post-cured in an oven under vacuum bag conditions using the same curing cycle applied to the Enduring-stage specimens during the experimental campaign reported in Deliverable D3.3.

Fracture toughness under Mode I loading conditions was evaluated according to ISO 15024 (Double Cantilever Beam, DCB), while fracture toughness under Mode II loading conditions was assessed following the EN 6034 standard (End Notched Flexure, ENF).

Interlaminar shear strength (ILSS) was evaluated according to the ASTM D2344 short-beam shear test method. Unlike the slotted Single Lap Shear test used in the experimental campaign reported in Deliverable D3.3, the ASTM D2344 method allows the welded region to be evaluated at multiple locations along the bonded area, since up to eight short-beam specimens can be extracted from a single welded coupon with dimensions of 120×25 mm². After post-curing, the welded coupons intended for ILSS characterization were cut using a waterjet system. During this cutting operation, several specimens separated spontaneously at the welded interface (**see Figure 26**), making it impossible to determine the interlaminar shear strength in those cases and consequently reducing the number of valid tests available for each welded coupon, as reported in Table 7. This behaviour clearly indicates poor adhesion between the heating element and one of the adherends, most likely caused by a non-uniform pressure distribution or by temperature inhomogeneities during the welding process. The exact origin of this variability has not yet been fully identified and will be the subject of further investigation during the next stages of the project.

Microstructural characterization was performed by preparing cross-sections of the welded joints and acquiring optical micrographs. Three equally spaced cross-sections were analysed for each welded specimen.

A total of three welding repetitions were produced for each mechanical test method.

The ILSS results obtained from the testable specimens are reported in **Table 7.** It is worth noting that, although all failures were interlaminar in nature and therefore acceptable according to the ASTM D2344 standard, most failures did not occur within the welded interface itself but rather within the laminates. This observation is particularly significant considering that the maximum shear stress during the short-beam test is expected to occur at the mid-thickness of the specimen, corresponding to the welded interface due to the symmetrical thickness of the adherends. Therefore, it can be concluded that the values reported in **Figure 27** are conservative and likely underestimate the actual strength of the welded joint.

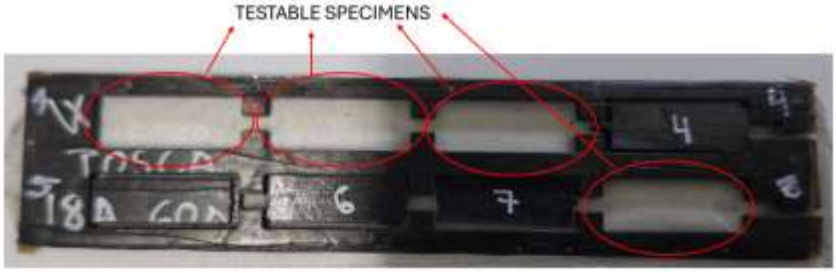

Figure 26: Picture showing the loss of specimens during waterjet cutting

	Number of testable specimens (testable/total)	Mean value (MPa)	Standard deviation (MPa)
Rep1	4/8	37.1	1.8
Rep2	7/8	42.5	10.4
Rep3	4/8	33.9	3.9
Overall	15/24	37.8	4.3

Table 7: Interlaminar shear strength results.

On the other hand, highly unsatisfactory results were obtained from the Mode I and Mode II fracture toughness tests. The measured values in terms of energy release rate of the fracture initiation are reported in Table 8. As can be inferred both from the low energy release rate values and from the inspection of the fracture surfaces after separation of the adherends (**Figure 28**), virtually no effective bonding was achieved between the laminates. Indeed, the fracture surfaces appear largely clean after separation, indicating that little or no interfacial adhesion was developed during the welding process.

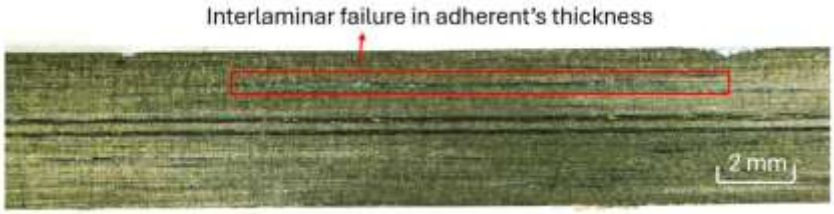

Figure 27: Picture showing the failure location in ILSS specimen.

These results highlight the poor quality of the joints obtained in the specimens manufactured for fracture toughness characterization, most likely as a consequence of the limited consolidation pressure that could be applied when welding specimens of these dimensions. As discussed in the study on the reprocessability of the 3R vitrimer resin reported in Deliverable D3.3, consolidation pressure was identified as a critical parameter for achieving satisfactory bonding between laminates. The lower pressure level adopted for the manufacture of the fracture toughness specimens therefore likely prevented the establishment of sufficient intimate contact at the interface, resulting in the extremely low fracture toughness values measured.

	Mean value (J/m2)	Standard deviation (J/m2)
GIc	24.5	5.3
GIIc	46.8	23.3

Table 8: Results of Mode I and Mode II critical energy release rate fracture initiation.

Finally, the microstructural analysis performed on cross-sections of the welded joints provided encouraging results. For each welding trial (three repetitions in total), three micrographs were acquired from equally spaced sections along the specimen length. In all cases, no visible discontinuities were observed between the heating element and the adherends that could indicate the presence of extensive unbonded regions or complete lack of adhesion.

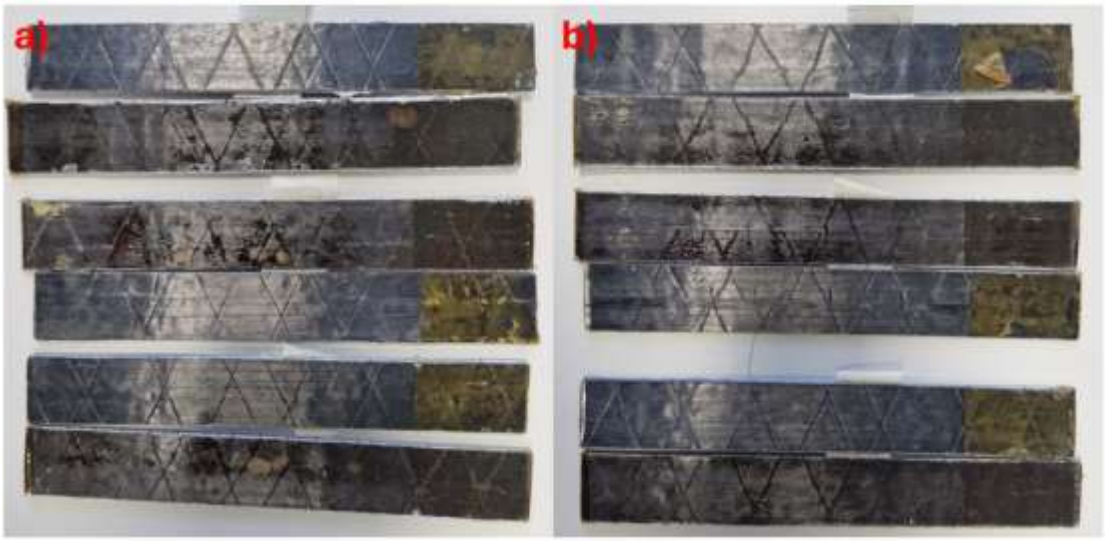

Figure 28: Picture of the joined surfaces after a) DCB and b) ENF testing.

The average porosity values measured within the welded region are reported in **Table 9.** An example of a representative micrograph is shown in **Figure 29**, where porosity can be observed mainly within the sandwich structure of the heating element itself, while only a limited amount of voids is present at the interface between the heating element and the adherends. These observations suggest that, despite the limitations identified through fracture toughness testing, a generally good level of interfacial contact was achieved over most of the bonded area, with defects being predominantly confined to the heating element rather than concentrated at the welded interfaces.

	Mean value (%)	Standard deviation (%)
Rep1	4.1	1.0
Rep2	4.7	0.5
Rep3	5.9	0.3
Overall	4.9	0.3

Table 9: Porosities percentages in correspondence of the joint.

Figure 29: Example of micrography of the welded joint's cross-section

As can be observed from the results obtained in this intermediate coupon-level demonstrator, the resistance welding of laminates based on the 3R vitrimer resin in the Enduring stage shows promising potential. The mechanical characterization carried out within this study demonstrates that it is possible to achieve welded joints with a measurable and, in some cases, significant level of mechanical performance. Nevertheless, there remains considerable room for improvement, particularly with regard to the repeatability and robustness of the process, as highlighted by the relatively large scatter observed in the mechanical test results.
For this reason, the activities planned for the second phase of the TOSCA project will focus not only on improving the mechanical performance of welded joints, but also on increasing process reliability and consistency. In particular, efforts will be devoted to the development of enhanced welding equipment capable of applying higher consolidation pressures during the joining process, since pressure has been identified as one of the key parameters governing bond formation in the 3R vitrimer system. In parallel, significant attention will be given to the development of a quality monitoring and process control strategy, aimed at ensuring more stable processing conditions and reducing variability in joint quality. These developments are expected to contribute to the establishment of a robust and industrially viable welding process for vitrimer-based composite structures in future aerospace applications.

4.5 Repair process

This section demonstrates repair processes adapted to vitrimer-based thermoset composite materials and evaluates their feasibility and effectiveness for restoring laminate integrity.

4.5.1 Methodology

The repair concepts are led and implemented by GMI, while ÉireComposites is responsible for carrying out experimental testing and evaluation of repaired panels to generate representative, coupon-level evidence. Repair trial activities commenced with the delivery of repaired panels from GMI to ÉireComposites, together with the associated process descriptions and repair context. The repaired panel is currently onsite at ÉireComposites and provides a realistic substrate for experimental evaluation of repair feasibility and compatibility with the recyclable thermoset system demonstrated within Deliverable D5.1.
ÉireComposites is carrying out experimental evaluation of the repaired panels using a defined set of coupon-level test methods. The assessment consists of non-destructive testing (ultrasonic C-scan inspection) and mechanical testing (tensile testing). Testing is intended to provide intermediate-level insight into repair integrity, material response, and practical implementation considerations, rather than final mechanical qualification or certification.

Regarding the repair processes GMI will use existing equipment that is currently in use in real life repairs on aerospace structures. This mainly involves ANITA 4.0 hot bonder, LESLIE machining toolkit and OLGA portable positive pressure application unit. The goal is to stablish a novel repair methodology for the new vitrimer composite materials. Within the framework of TOSCA project two different scenarios will be tested:

Scenario 1: Repair cosmetic or structural damage **without patch**, by exploiting the innovative self-healing capability of the new 3R vitrimer resin (TS-1 material system). Initially artificial damages will be created by impact at different energy levels on a composite panel. The panel will be inspected by ultrasonics (A-scan) in order to characterize the area and size of the damages. After inspection the panel will be repaired by only applying heat and pressure. For the validation of repair, the panel will be inspected again using ultrasonics (A-scan) in order to assess the degree of repair.

Scenario 2: Repair of severe damage **using patches** made from vitrimer pre-preg. In this scenario two different cases will be tested:

- Case 1: Bonding the patch on the test panel **using 3R vitrimer resin** as adhesive**.**
- Case 2: Directly bond of the patch **without the use of adhesive**.

In both cases the process starts by removing the "hypothetical damaged layers" of composite material and create a typical stepped contour using LESLIE toolkit. The next step is to fill the area using vitrimer/carbon fibre pre-preg as the patch, respecting the orientation of the fibres. The patch will be cured and bonded by applying the appropriate curing cycle (ANITA 4.0 hot bonder) and external pressure (OLGA portable positive pressure application unit). After the repair process the panels will be tested in order to validate that they have been repaired. The test panels will be cut in smaller samples (strips), which will be mechanically tested under tensile or three-point bending loading. The comparison between the strength of the un-repaired and repaired samples will give the final estimation of the degree of repair.

4.5.2 Results

Scenario 1: Repair cosmetic or structural damage without patch
For this scenario a composite panel made by AFP method at FIDAMC was used as the test sample. The panel was sent to CIDETEC to perform impact test at different energy levels, as illustrated in **figure 30.**

The experimental setup involves the use of appropriate heating blankets, hot bonder ANITA for controlling and monitoring the heat process, a vacuum pump for applying negative pressure inside the vacuum bag and OLGA pressurization system for applying positive pressure. In the following figures (**31 and 32)** the experimental setup is presented and described analytically:

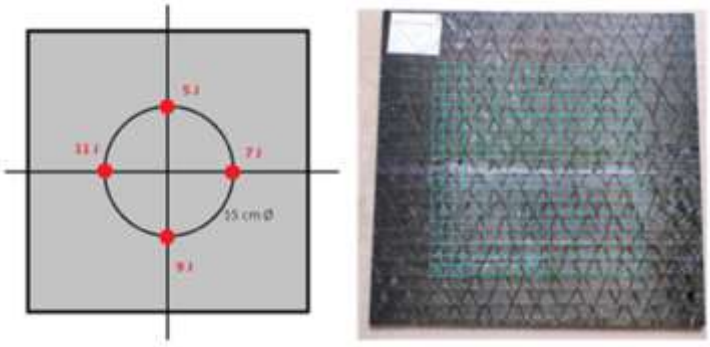

Figure 31: Schematic representation of the location and impact energy on the test sample.

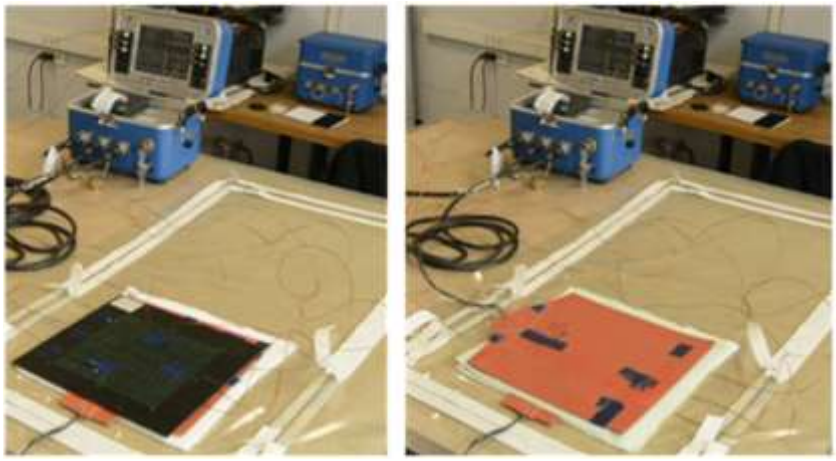

Figure 30: Installation of thermocouples and heating blankets on the back and on top of the composite panel

The heat cycle involves a first plateau at 90 °C for 60 minutes and a second plateau at 190 °C for 45 minutes. The application of additional pressure of 5 bars starts at 50 °C remaining constant during the cycle and removed after the completion at 55 °C. During the repair process the temperature from the thermocouples, the pressure inside the vacuum bag and the % power of each heating zone is recorded and presented in **figure 33.**

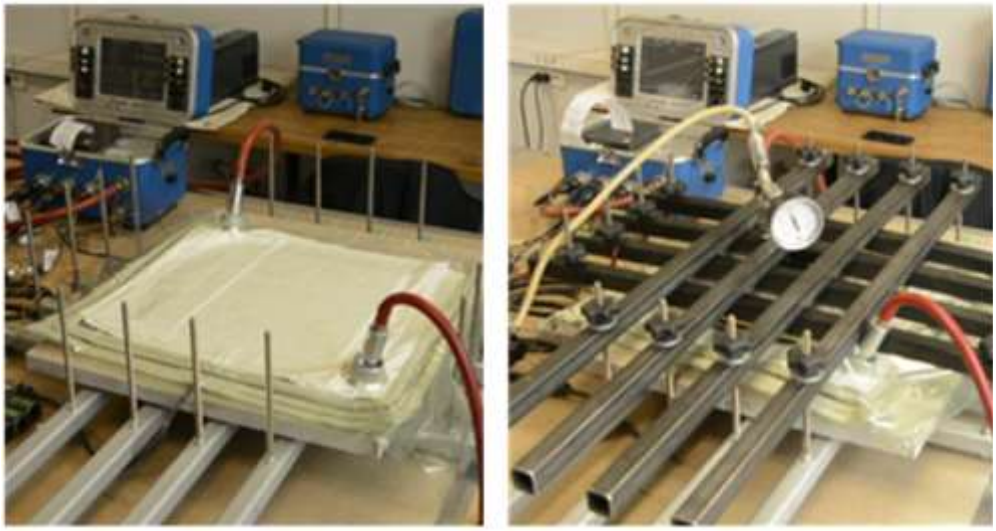

Figure 32: The panel inside the vacuum bag and OLGA pressurization system for applying positive pressure.

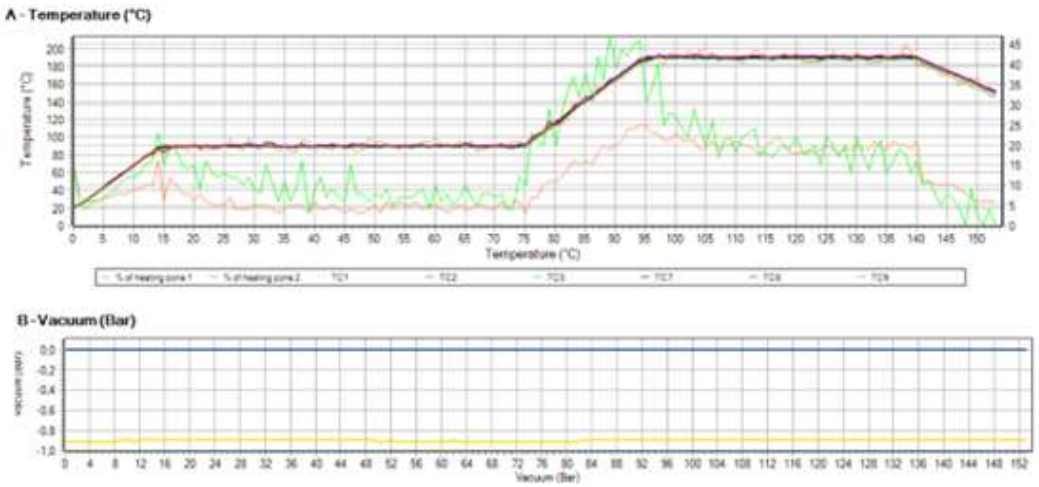

Figure 33: Measurements from the thermocouples, the pressure inside the vacuum bag and the % power of each heating zone

Before the application of heat and pressure the panels were inspected using ultrasonics (A-scan). The surface of the panel is divided in smaller squares (1x1 cm) by a 20x20 grid. Each square is inspected for damage. The results before and after the repair process are presented in **figure 34.**

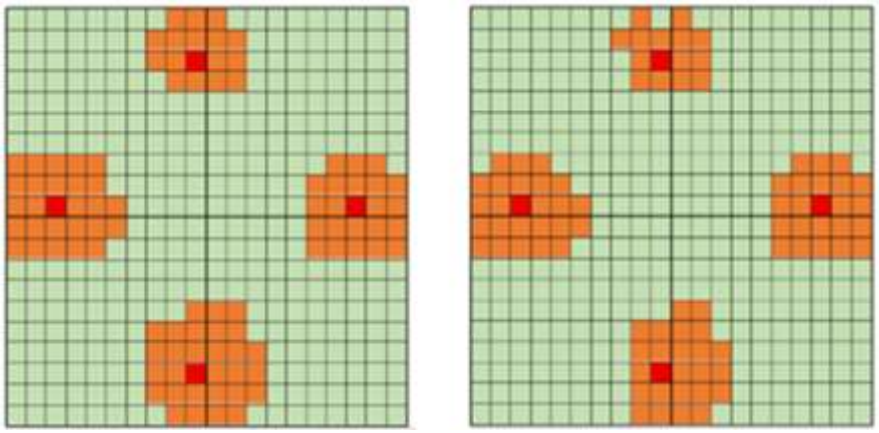

Figure 34: The results from the ultrasonic inspection before and after the application of heat and pressure

The results from the ultrasonic inspection showed poor degree of repair. In most cases there was not a reduction of the size of the damage. This the first attempt showed that the applied temperature or pressure or both were not sufficient to activate the repair mechanism of the vitrimer matrix. In the following tests higher temperatures will be tested in order to define the minimum activation temperature

Scenario 2: Repair using patch made from vitrimer pre-preg

For this scenario two composite panels made by AFP method at FIDAMC were used as test samples. In both cases the first step is to remove the "hypothetical damaged layers" of composite material and create a typical stepped contour using LESLIE toolkit, as illustrated in **figure 35**.

Figure 35: The LESLIE toolkit used to create a typical stepped contour

Case 1: Bonding the patch on the test panel using 3R vitrimer resin as adhesive

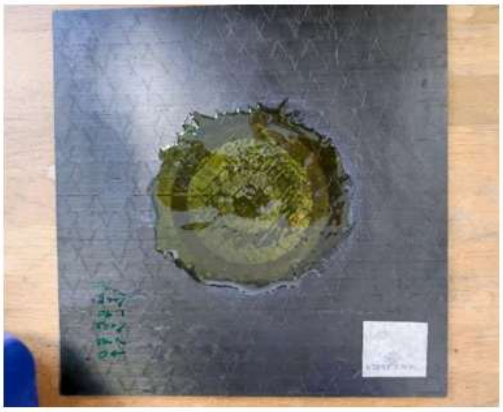

Figure 36: The 3R resin in liquid form used for bonding the patch

Figure 37: The patch prepared from carbon fiber/ 3R resin pre-preg

In this case the bonding of the patch is made by using the 3R resin as adhesive (**figure 36**). The preparation involves:

- Weigh of the required quantities of resin (Part A) and hardener (Part B) separately by ratio 100 parts of Part A + 50,4 parts of Part B
- Heat application on the part B at 85°C until it is fully melted.
- Heat application on the Part A at 40°C in order to lower the viscosity.
- Addition of the Part B on the Part A and mixing.
- The mixture is ready for the use.

The patch was prepared from carbon fibre/ 3R resin pre-preg sheets on the "enduring state". The fibre orientation of the patch was made in respect of the fibre orientation of the composite panel, as illustrated in figure 37.

Case 2: Directly bond the patch without the use of adhesive

In this case the bonding of the patch is without the use of adhesive. The patch was prepared from carbon fibre/ 3R resin pre-preg sheets on the "enduring state". The fibre orientation of the patch was made in respect of the fibre orientation of the composite panel, as illustrated in **figure 38.**

Figure 38: The patch prepared from carbon fiber/ 3R resin pre-preg

In both cases the experimental setup (**figure 39**) involves the use of appropriate heating blankets, hot bonder ANITA for controlling and monitoring the heat process, a vacuum pump for applying negative

pressure inside the vacuum bag and OLGA pressurization system for applying positive pressure. In the following figures the experimental setup is presented and described analytically.

Figure 39: the experimental setup for curing the patch in both cases

The patch was cured and bonded by applying the appropriate heat and external pressure. The heat cycle involves a first plateau at 90 °C for 60 minutes and a second plateau at 180 °C for 30 minutes. The application of additional pressure of 5 bars starts at 50 °C remaining constant during the cycle and removed after the completion at 55 °C. During the repair process the temperature from the thermocouples, the pressure inside the vacuum bag and the % power of each heating zone is recorded and presented in **figure 40**.

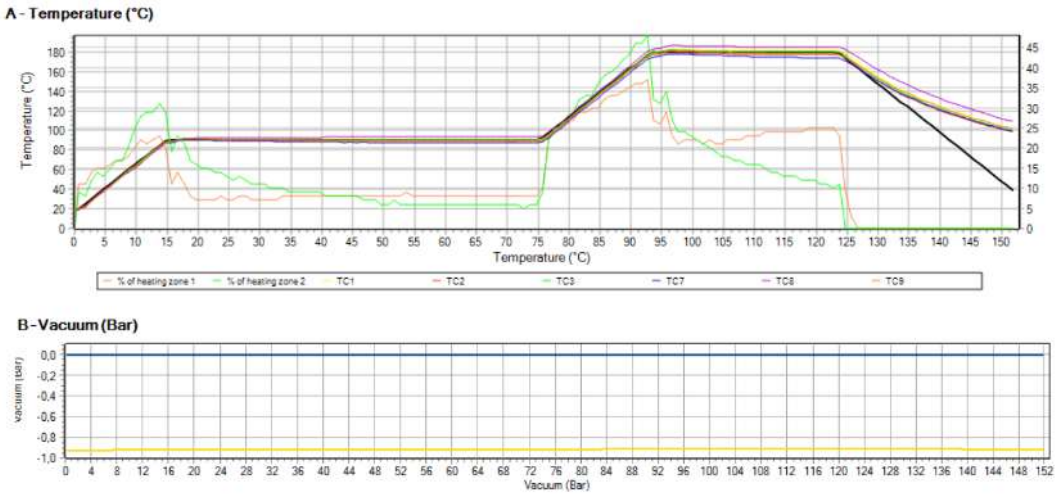

Figure 40: Measurements from the thermocouples the pressure inside the vacuum bag and the % power of each heating zone

After completing the repair process the panels were visually inspected for any defects. In case 1 there is a small misalignment of the patch that was caused by a slight movement due to excess of adhesive. The bonded patches are presented in **figure 41**.

Figure 41: the composite panels after the repair. Case 1 on the left, case 2 on the right

Repair validation activities within this work focus on the experimental evaluation of repaired composite panels, with the objective of assessing the feasibility and quality of repair implementation on vitrimer-based laminates. The repair concepts and execution were carried out externally, with the work presented here focused on the inspection and mechanical evaluation of repaired specimens at coupon level.

Two repaired panels were received for evaluation, corresponding to components EC-RD-4137 and EC-RD-4138. Both panels were subjected to non-destructive testing (NDT) using ultrasonic C-scan inspection upon receipt, with the aim of assessing the internal condition of the repaired regions and identifying any defects that may influence subsequent mechanical performance.
The NDT results (**figure 42**) indicated that Panel EC-RD-4137 exhibited significant signal variation and indications of defects not directly attributable to the repair itself, making it difficult to isolate and assess

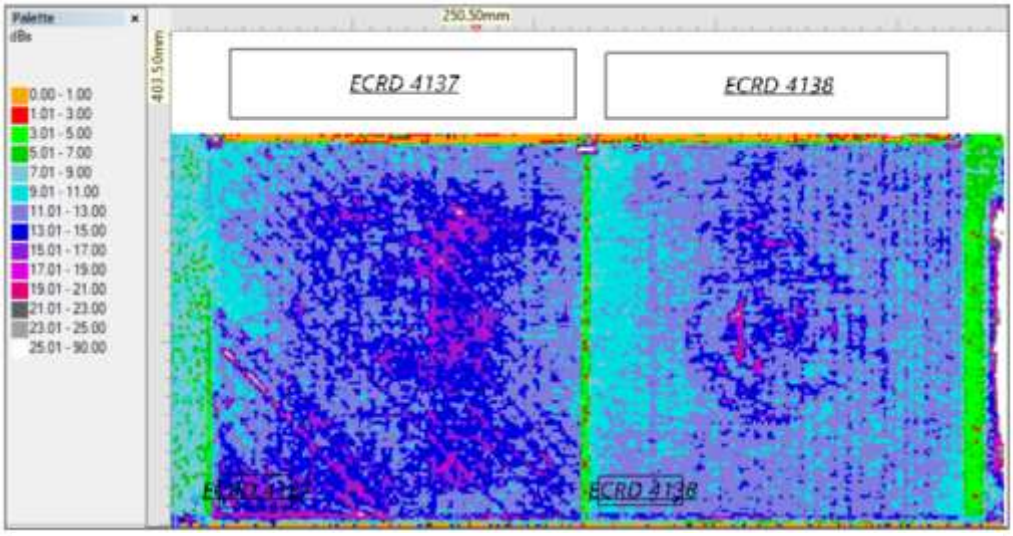

Figure 42: NDT Test results from the two panels repaired by GMI

the effectiveness of the repair. Variability in the panel response suggests the presence of underlying laminate inconsistencies, reducing confidence in direct interpretation of repair quality from NDT data alone. Panel EC-RD-4138 demonstrated a more consistent ultrasonic response across the majority of the laminate; however, indications of defects were still observed within the repaired region. While this panel showed improved uniformity relative to EC-RD-4137, the inspection results do not provide conclusive evidence of a defect-free repair.

These findings highlight a key challenge in the evaluation of repair effectiveness within this study, namely the influence of pre-existing laminate variability. As observed in earlier sections, variability in the base laminate can obscure the distinction between defects originating from the original panel and those introduced during the repair process, limiting the interpretability of inspection data.

To further assess repair performance, both panels have been submitted to the Composites Test Laboratory (CTL) for tensile testing in accordance with ASTM D3039. Specimens are machined across the panel width from the centre outwards, as illustrated in **Figure 39**, such that test coupons are extracted both within the repaired region and from the surrounding parent laminate. This approach enables direct comparison between the repaired zone and the base material, while also providing multiple specimens from equivalent regions to assess repeatability and variability within the repair.

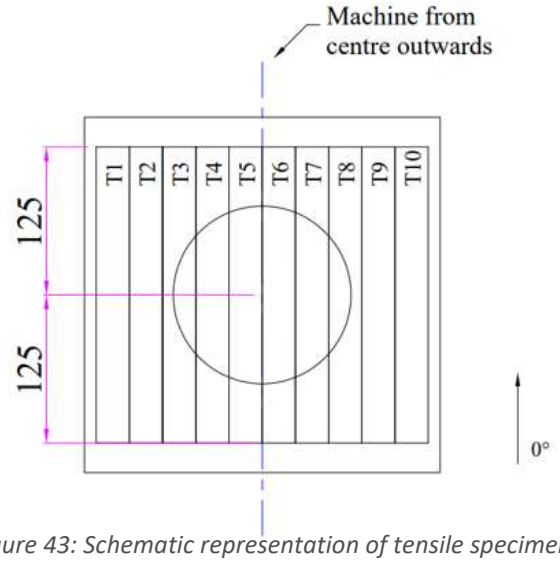

Figure 43: Schematic representation of tensile specimen extraction across repaired panel, showing machining strategy from centre outwards and specimen distribution relative to the repair zone.

This specimen extraction strategy is particularly important given the variability observed in the NDT results, as it allows mechanical testing to be used to further differentiate between repair quality and underlying laminate inconsistencies. In addition, comparison against specimens extracted from virgin panels will provide a baseline reference for evaluating the effectiveness of the repair.

At the time of writing, tensile testing is ongoing and results are not yet available. As such, a quantitative assessment of repair performance cannot yet be made. However, the work completed to date demonstrates the successful implementation of a structured evaluation approach, combining NDT inspection and mechanical testing to assess repair quality at coupon level.

From an assessment perspective, repair implementation has been successfully demonstrated at coupon level, with appropriate inspection and testing methodologies established. However, the current dataset does not allow for a definitive evaluation of repair effectiveness due to the combined effects of underlying laminate variability and the absence of completed mechanical test results. Further evaluation, including correlation between NDT data and tensile test results, will be required to fully assess the structural performance of the repaired regions and the consistency of the repair process.

4.6 SHM integration

This section demonstrates the integration and functionality of structural health monitoring sensors within composite structures manufactured using the developed vitrimer-based materials.

4.6.1 Methodology

In the case of SHM using the magnetostrictive sensors the methodology will be similar to the one described in deliverable D4.3. Initially the magnetostrictive ribbons will be surface mounted on composite panels using epoxy adhesive and cured at room temperature. For the intermediate demonstrator two different composite panels will be prepared:

- Using commercial grade composite laminates (Carbon/Epoxy)
- Using 3R resin /Carbon fibre tapes

Choosing two different composite materials for the test panels gave a better overview of the performance of this SHM method.

After the fabrication of the panels, the inspection will be carried out by ultrasonics (A scan) and the inductive transducer combined with the motorized system, described in D4.3. This system records the position as well as the output from the transducer and the data are collected and stored on a txt. file from which a 3D graph is generated and will be the reference of the “healthy” state of the panels.

Then the panels were be subjected to drop weight impact test at different energy levels at different locations in order to create artificial damages. In order to validate the sensitivity of this method, the samples were inspected again using ultrasonics (A scan) and were scanned by the motorized system. The any irregularities in the reference measurements from the magnetostrictive sensors after the impact, should coincide with the location and the size of the damage identified by the ultrasonic inspection.

The main objective of the SHM system at the intermediate stage of the project is to prove the ability of the developed acoustic emission system to identify, locate, and quantify impact events. For that purpose, eight 200x200mm flat panels were manufactured by manual lay-up using standard aeronautical grade pre-pregs of commercial material (M21E/IMA-12K), with mechanical and interlaminar characterization available at ITA. The stacking sequence envisioned for the final demo was followed achieving a thickness of 1.6mm. A sparse sensing network based on PVDF-TrFE transducers was surfaced-mounted on each specimen using 4 sensors in a “cross” arrangement. A DAQ system continuously monitors the voltage output from the transducers and records the signal from all channels each time any sensor trespasses a predefined threshold. An extensive experimental campaign was performed at sub-damage-threshold impact energies (0.25 to 1J) at different locations.

A complete data-processing pipeline has been developed, including signal filtering and cleaning, normalization, and feature extraction. Based on these features, two sequential models provide event localization and energy quantification.

First, a localization model—based on a supervised machine learning algorithm—is applied. The model uses the extracted features as inputs and predicts impact location on the specimen plane. This model is trained using labelled data (impact point coordinates) obtained during an experimental testing campaign designed for both training and validation.

Second, a model based on the electrical energy of the sensor signals has been developed for energy quantification. This model accounts for key factors such as the distance between each sensor and the impact point, the orientation of the propagation path relative to the material’s principal directions, and the temperature. The model parameters are derived from experimental measurements. To mitigate the variability observed experimentally—mainly due to the small size of the sample plate—a hybrid approach

is also implemented. In this framework, a machine learning model is trained to compensate for residual errors and improve the accuracy of the energy estimation

4.6.2 Results

For the fabrication of the test panels the magnetostrictive patch is bonded on the surface of the carbon fibre laminates. The magnetostrictive ribbons are placed in parallel on a thin fiberglass tissue and bonded using epoxy resin which is cured at room temperature, as illustrated in **figure 44.**

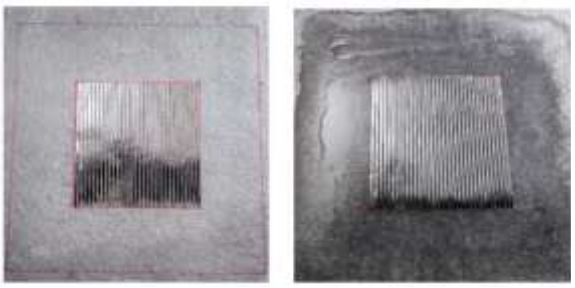

Figure 44: The preparation and bonding of the magnetostrictive patch

After the fabrication of the panels, inspection is carried out using ultrasonics (A scan) and also scanned by the motorized system. The inspection area is a rectangular of 8x8 cm divided by 1x1 cm grid and it is marked on the surface of the samples using a red marker, as illustrated in **figure 45**.

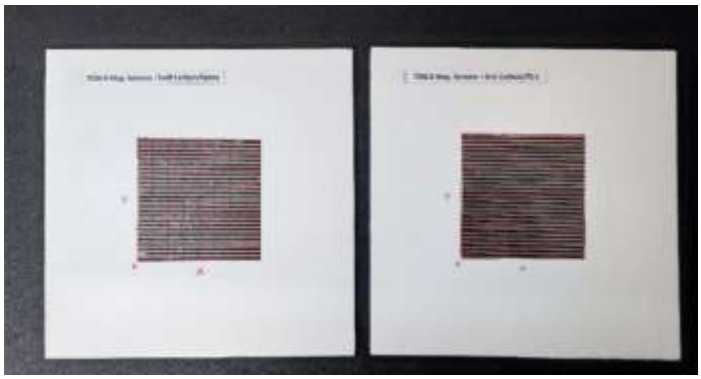

Figure 45: the test panels ready for inspection

The panels are subjected to drop weight impact testing on the facilities of ITA. The energy level is selected to 9 Joules for both cases. The location of impact is on the centre of the panel in both cases. Visual inspection after the impact shows damage (fibre breakage) at the back surface of the commercially grade panel. The samples are inspected again using ELISA instrument for ultrasonic testing (A scan). The comparative results from the ultrasonic inspection, before and after impact, shows damage after the impact, as illustrated in **figure 46**.

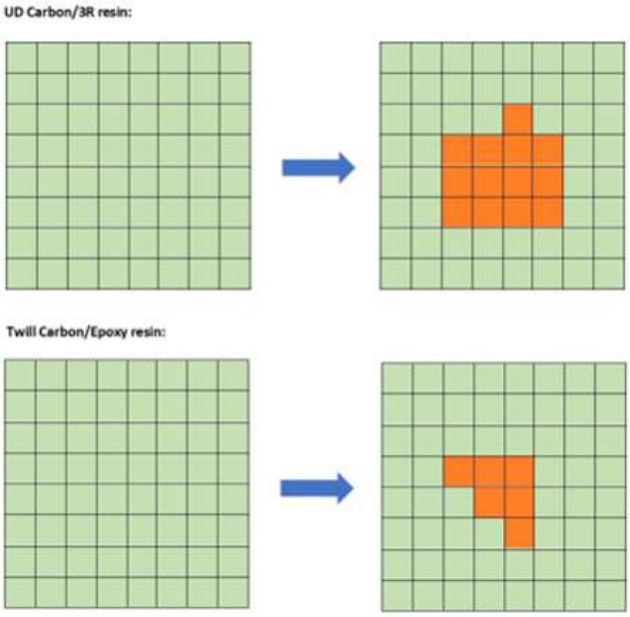

Figure 46: Results from the ultrasonic inspection, before and after impact.

The panels are inspected also using the motorized system over the magnetostrictive patch. The comparative results from the magnetostrictive patch, before and after the impact are illustrated in **figure 47**.

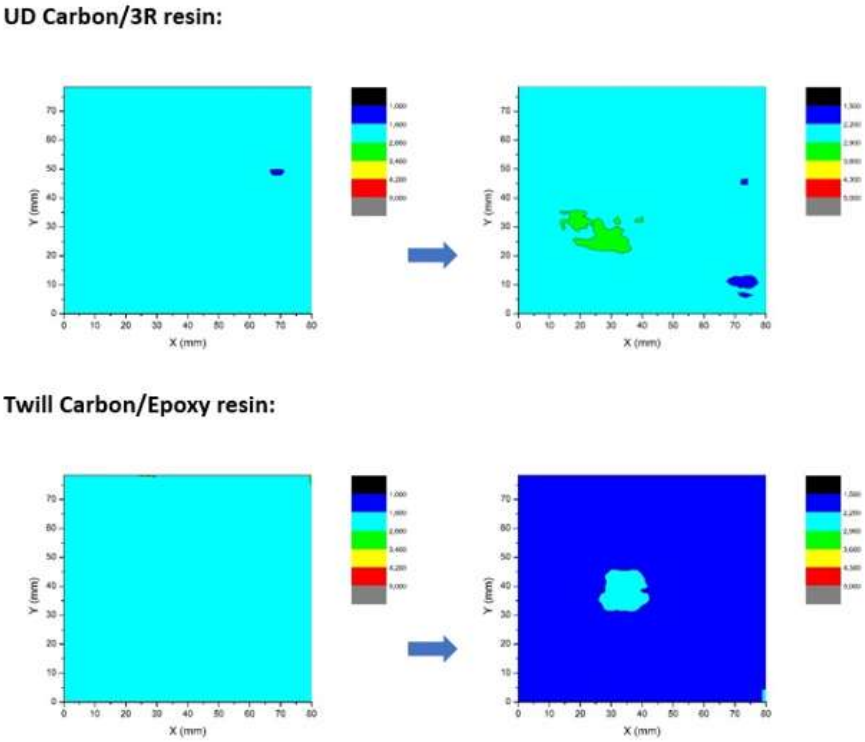

Figure 47: Results from the magnetostrictive patch, before and after impact.

The results from the magnetostrictive patch coincide with those from the ultrasonic inspection in the case of the commercially grade panel and partially in the case of 3R resin/Carbon panel. Future tests are expected to validate the performance of inspection using magnetostrictive patch. As it is presented also in the deliverable 4.3 this method should be able to detect the location and the size of the damage caused by impact.

The performance of the impact localization method is evaluated in terms of mean, minimum, and maximum error, defined as the Euclidean distance between the actual and predicted impact points. The evaluation is performed using a test dataset consisting of impact locations distributed within the training grid.

The next figure summarizes the error metrics grouped by energy level. A comparison is made between the full feature space and a reduced feature set, where features are selected based on physical relevance. Separate models are trained for each energy level and evaluated both on matching and non-matching energy levels, in order to assess the model's ability to generalize independently of energy content.

According to the results shown in the **Fig 48**, the best performance is achieved when training with the full dataset and testing on the complete set of energy levels. Under these conditions, the average localization error is approximately 19.8 mm (9.9% of the plate edge length) when using the full feature set, and 27.56 mm (13.8% of the plate edge length) when using the reduced feature set. For other training configurations, the mean error increases up to 37.5 mm (18.75% of the characteristic plate length in the worst-case scenario with the reduced feature space).

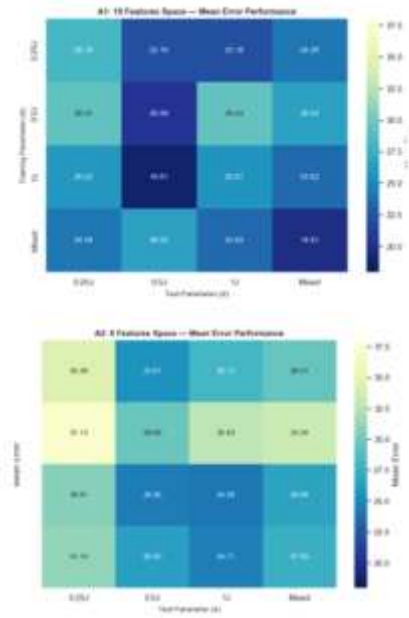

Figure 48: Mean location error comparison A1: full features space. A2: Reduced feature space

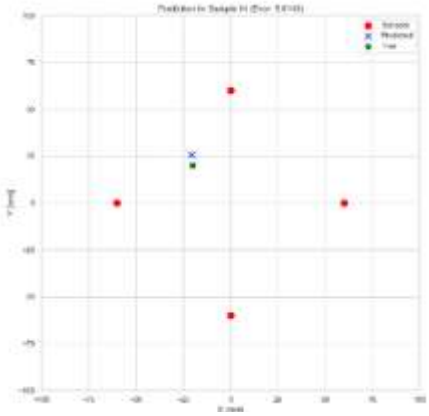

Figure 49: Impact localization results.

A graphical representation of the impact localization is shown in **Fig 49**, where sensor positions, actual impact points, and predicted locations are displayed.

The prediction error is lower within the region enclosed by the four sensors. This is due to the fact that the direct wave generated by the impact reaches the sensors without significant interaction with the plate boundaries. In contrast, boundary reflections significantly affect the waveform in other regions, increasing signal complexity and reducing prediction accuracy.

This explains why the full feature space outperforms the reduced one: it captures additional characteristics of the complex signals generated by wave interactions with the plate edges.

The results for impact energy quantification are divided into two parts. First, an uncertainty analysis of the experimental measurements is performed, as variability depending on the plate region is observed. Second, the results of the model fitting are presented in terms of predicted versus actual energy values

It is important to note that the impact energy levels are intentionally kept low to prevent any permanent damage to the plate. Improved accuracy is expected if higher energy levels are considered.

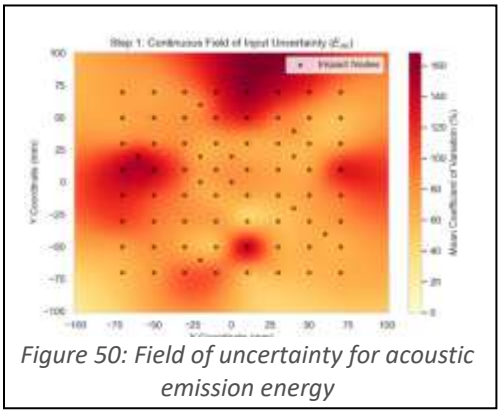

Figure 50: Field of uncertainty for acoustic emission energy

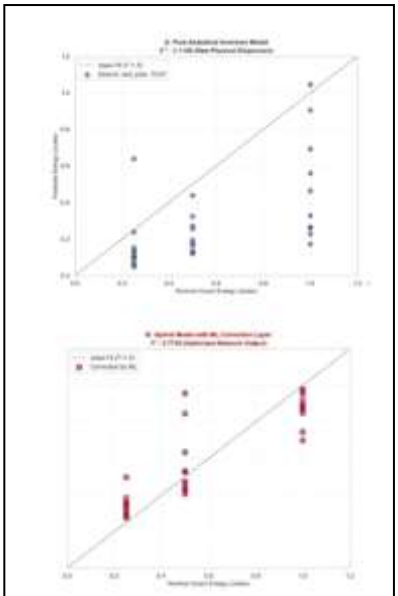

Figure 51: Predicted vs. actual impact energy for A) analytical model and B) hybrid approach

Figure 50 shows the distribution of the coefficient of variation of the acoustic energy for all impact tests conducted on the sample. It can be clearly observed that regions located behind the sensors exhibit a shadowing effect in wave propagation, resulting in increased signal variability. These areas of higher variability are likely associated with reduced sensor sensitivity.

Figure 51 presents the energy prediction results. Figure 51 (a) shows the predictions obtained using the analytical model, which is based on wave propagation physics and accounts for both the distance and orientation between the impact point and the sensors. Figure 51 (b) shows the predictions after compensating the analytical model error using a machine learning approach.

The mean prediction error is approximately 0.35 J for the analytical model, whereas the hybrid model reduces this error to approximately 0.11 J. This corresponds to a minimum relative error of approximately 11% at an energy level of 1 J.

4.7 Digitalization: data management & digital twin

This section demonstrates the acquisition, management, and integration of manufacturing and monitoring data into digital environments to support digital twin implementation.

4.7.1 Methodology

For the implementation of the digital twin a data model based on the HDF5 (Hierarchical Data Format) technology, which was selected for its proven capability to store large, heterogeneous, and hierarchically organized datasets efficiently. The implementation follows the **composite manufacturing database schema** developed by Dassault Systèmes, originally designed to ensure interoperability between simulation, manufacturing, and quality assessment tools. Within TOSCA, the schema has been adapted and extended to accommodate additional process and sensor data, thus enabling a continuous digital thread that links material geometry, process data, and resulting component quality through damage and repairs. It has been also further extended to include repair and joining process data, as collected by corresponding state-of-the-art equipment, focusing on the TOSCA developed vitrimer resins.

HDF5 (Hierarchical Data Format version 5) is a binary, platform-independent file format designed for storing large and complex datasets, originally developed at the U.S. National Center for Supercomputing Applications and now maintained by the HDF Group. Its fundamental concept is a hierarchical data model composed of groups (similar to directories) and datasets (multi-dimensional arrays), complemented by attributes for storing metadata. This model enables users to construct structured, nested representations of engineering information, where each element can contain numerical arrays, strings, compound types, or references to other parts of the file. Such structural flexibility is essential for describing composite components, which combine geometry, materials, ply definitions, process parameters, and inspection results within a single coherent file.

The Dassault Systèmes Composite HDF5 Scheme is organized around two main top-level groups: /composite_manufacturing and /composite_cae. Together, these groups provide a unified data structure for representing both the as-manufactured component and its corresponding simulation model within a single HDF5 file. This separation ensures a clear distinction between manufacturing-driven information and finite element (FE) analysis data, while allowing both domains to reference shared geometry and material definitions when required. The/composite_manufacturing group is the central container for all information derived from design, lay-up, inspection, and process monitoring

At the current stage of the project (i.e. coupon level demonstrations), it is not yet relevant to demonstrate the acquisition of monitoring data, as most of the specific data is only now being acquired or the process to do so will change significantly over the course of the remaining project and during the transition from coupon level to demonstrator level.
What we can and will present at this point, however, is how the already gathered – mostly non demonstrator specific – data is stored and structured inside the manufacturing database. The data, to large parts already described in deliverables D3.4 and D4.4, can be presented visually by the use of a GUI, specifically developed for the project and its digital twin platform. The GUI allows navigating the manufacturing database and to visually display geometric information such as the individual plies manufactured, together with process information spatially related to specific regions of the part. This includes temperature curves of areas repaired or joined, and defects that occurred during lay-up. Screenshots and videos will be taken of the software and GUI to demonstrate the usability of the manufacturing database.

The specimens manufactured for the SHM evaluation campaign were also used for evaluating the impact damage prediction models. An experimental campaign of increasing energy impacts, from 1J up to 20J, was performed at different positions of the plates.
Active thermography was used to inspect the plates before and after the tests to ensure structural integrity and identify any initial subsurface defects. In parallel, Finite Element Method (FEM) models were developed (**fig.52**) to replicate the exact specifications of these physical plates. Identical impact test was then conducted on both the physical specimens and the numerical models. By correlating the experimental data with the simulation outputs, a comprehensive comparative analysis was performed to evaluate the predictive accuracy of the FEM models and the influence of material consistency as observed through the initial thermographic mapping.

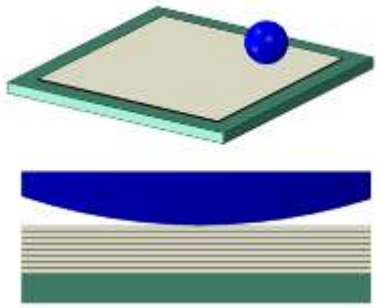

Figure 52: FEM model of the laminate panel on the foam and the spherical impactor.

4.7.2 Results

The main result obtained from the FEM simulations is the damage prediction in the laminate panel under different impact energies.
Simulations were performed using Abaqus/Explicit, as it enables dynamic analyses with a reasonable computational cost. Resembling the experimental specimens manufactured for the intermediate validation of SHM methodologies (see Section 4.6.1) a FE model was built including all the composite material layers, as well as very thin intermediate layers representing the interfaces between plies, which have been modelled using cohesive elements.

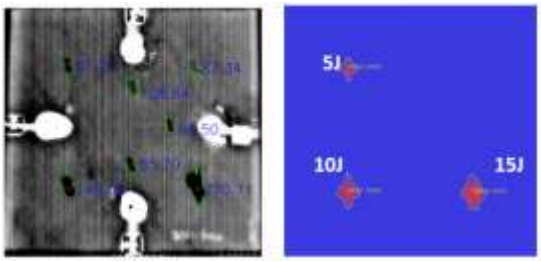

Figure 53: Thermography after impact and damage prediction for impacts with different energies

From the simulations, the damage variable (SDEG) of the cohesive elements is obtained, allowing the identification of whether delamination has occurred between each pair of plies. 49 shows the thermography of a plate that has been subjected to impacts at different energy levels, along with the damage predictions obtained through finite element modelling (FEM) for impact energies of 5, 10, and 15 J.

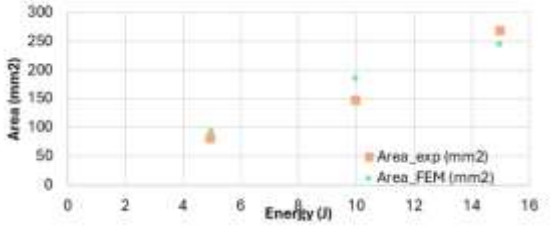

Figure 54: FEM prediction Vs experimentally measured damaged area after impact.

A threshold value of damage was selected to be plotted cumulatively. This means that, in 53, it is possible to observe the extent of the damage in the composite and also to obtain a qualitative idea of the damage level across the entire surface. The more intense the red colour is, the more layers have been damaged. These predictions can be compared to the experimental observations (Fig 54).
Finally, a Python script was developed to transfer information from these simulations into the Database in .h5 format. The data stored in the database include the model geometry (nodes and elements), material properties, and damage maps (Fig 55).

Figure 55: Example of the database structure for the CAE model

4.8 Recycling processes

This section demonstrates the recyclability of the developed vitrimer-based thermoset composite materials and validates the recycling process at laboratory scale.

4.8.1 Methodology

The approach used to demonstrate the recyclability of the composites produced with TS-1 vitrimer at laboratory scale consisted of the development of two main activities:

- Definition of the requirements of the recycling process (Developed in T2.3. and reported in D2.2). The technical objectives to be met by the recycling process were defined. Economic, logistical and

certification aspects were also defined, incorporating the requirements needed to enable efficient and scalable composite recycling.

- Definition of the recycling process at laboratory scale (Developed in T3.5 and reported in D3.1). In the initial phase, the recycling process of neat TS-1 vitrimer was studied to stablish the most suitable conditions. Next , the optimization for the composite produced with TS-1 vitrimer was initiated, starting at the laboratory scale with small-scale tests.

The fabrication of composites by compression molding technology is a common method for producing composite materials with specific shapes and properties (**Fig. 57**). This process often involves combining reinforcing fibers and particles with a matrix material and then compacting the mixture (in this case vitrimer based scraps) into a mold under pressure. The challenges with the fabrication of the composite components containing recycled materials fractions cover following aspects connected with especially different size and geometries of scraps, comparably high viscosity of the system during remelting, possible necessity of dosage additional amount of resin into system in order to improve quality of the plates etc. Below it is specified general overview of the fabrication process by means of pressing material into the molds for fabrication of plat plates as preliminary composite scraps based on vitrimer resin proof of concept. The composite manufacturing process began with the selection of composite scraps delivered by the project partners in the form of vitrimer cured wastes from tapes production as well as prepregs with different defects and in the state out of date (**Fig. 56**). The reinforcement phase consisted of carbon. The waste materials were prepared in advance by cutting process into smaller size pieces. The mold was designed to be made of metal to provide sufficient mechanical strength, dimensional stability, and durability during the forming process. The prepared mixed material was heated up and subsequently pressed in the mold. The parameters for compression molding preprocessing of vitrimer based were as follows (Table 10).

Figure 57: Press for fabrication of composites containing vitrimer based wastes.

Figure 56: Vitrimer based wastes placed in mould.

Short name	Additional resin [%]	Waste material [%]	Mass [g]	Pressing parameters [time/temperature/pressure]
TS 1/26	0	100	256.57	Pressure= 50 tones c.a. 62,7bar; I. Time 1 h | Temp= 90°C; II. Time 0,5 h | Temp= 180°C
TS 2/26	0	100	275.83	Pressure= 50 tones c.a. 62,7bar; I. Time 1 h | Temp= 90°C; II. Time 0,5 h | Temp= 180°C
TS 3/26	0	100	261.43	Pressure= 50 tones c.a. 62,7bar; I. Time 1 h | Temp= 90°C; II. Time 0,5 h | Temp= 180°C

Table 10: Preprocessing parameters of vitrimer cured wastes by means of compression molding

The applied pressure compacted the material and ensured close contact between the wastes and the epoxy matrix, reducing voids and improving consolidation. After pressing, the composite underwent curing in the temperature range delivered by the CIDETEC. This step is essential to achieve the maximum mechanical strength and stability of the final product. Once the pressing and curing stages were complete, the

composite plate was allowed to cool. After cooling, the component was removed from the mold, and any excess material were machined to obtain the required final geometry. At the end of the process, post-processing was performed.

4.8.2 Results

Definition of the requirements of the recycling process: Chemical recycling process was chosen as the process to be studied by CID in the project, as it aims not only to recover the carbon fibres but also to revalorize the epoxy vitrimer matrix. The process consists of two stages. Firstly, an appropriate solvent swells the vitrimer and separates the laminate plies, dissolving part of the vitrimer. Secondly, the vitrimer remaining in the plies is dissolved by the use of a disulfide-containing agent, which reacts with the vitrimer's disulfides under relatively mild conditions. The preservation of the Tg of the recovered vitrimer and the integrity of the fabric will depend on the proportion of vitrimer dissolved during each step and the stirring conditions required. Main specifications were defined for the fibres and vitrimer to be recovered from the chemical recycling.

Specification		Value
Carbon fibre	**Fabric structure**	The same as that of virgin fabric
	Maximum residual vitrimer content	5%
	Mechanical properties	≥90% of the original value
Vitrimer	**Reprocessability**	Second generation sheet
	Tg (°C)	90% of the original value
	Recovered vitrimer from original composite	50% of the original content

Table 11: Specifications of the recovered fibres and vitrimer from panels produced with TS-1 formulation

Definition of the recycling process at laboratory scale: Firstly, the recycling process of neat TS-1 vitrimer showed that the N-Butyl-2-pyrrolidone (NBP) was the most appropriate solvent, while two agents, one containing a disulfide group and the other a thiol group, were chosen to continue the process at the composite level, with specimens of 20x20 mm. At that point, maintaining the fabric structure was not considered a priority, but rather defining the optimal parameters to obtain vitrimer-free fabric. The study concluded with the selection of the disulfide-containing agent and defining the process parameters in terms of temperature and time. The recovery of vitrimer-free fibre was confirmed by SEM analysis (Fig.58). Full recovery of the vitrimer from the solvent could not be achieved due to the small size of the laboratory-scale specimens. Being demonstrated the complete dissolution of the vitrimer from the composite, in WP6 the process will be scaled up to recover both the fabric (with its original structure) and the vitrimer.

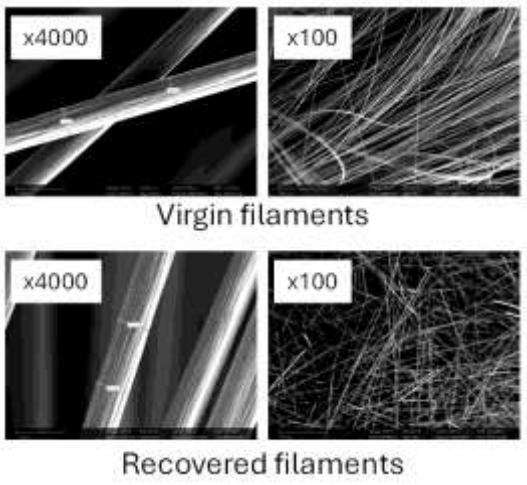

Figure 58: SEM images of virgin and recovered vitrimer-free carbon fibre filaments

In the first stage of NOMA's preparation for multirecycling process materials in the form of vitrimer based cured (enduring stage) tapes and uncured (tacky) wastes of prepregs roles provided by the partners were characterized (**Fig.59**) in order to find proper approach for further treatments. The typical geometry of pieces was measured and common structure of cut offs was characterized by means of microscopic techniques. What was characteristic for all investigated materials, carbon fibers constituted the reinforcement phase. In Table 12 all characteristic parameters for received different types of materials were collected including quantity of material obtained from partners in the first delivery package. In total 5 different types of wastes were obtained including one roll of uncured prepreg with lower than designed amount of resin, as well as cut offs from tapes production in cured state.

Figure 59: Typical vitrimer based wastes, on the left uncured prepregs, on the right cured types.

Type and name of scraps	Shape	Thickness [mm]	Width [mm]	Length	Mass [kg]/ quantity
1 roll of prepreg produced with UD CF and epoxy vitrimer, TS1-PP-2- AIMEN-	rectangular shape	~0,2	300	70 lineal metres	10,540, 70 lineal metres
Scraps of prepreg produced with TS-1 formulation in enduring stage	different shapes, rectangular shape	~0,2	~300	x	2,7
Scraps of prepreg produced with TS-1 formulation in enduring stage	long, narrow strip	~0,2	11-13	x	0,053
Uncured material- reference of the material is TS-1-PP6	long, narrow strip	0,20-0,23	11-15 /26	x	0,146
Autoclave scraps with delaminated and pore like spaces between the layers	different shapes	1,30-2,90	x	x	0,329

Table 12: Parameters of vitrimer based wastes collected from the project partners

Additionally, microscopic observations (light and SEM) of delivered materials were conducted to observe their structure, fibres aligment as well as integrity. In the Fig. 60, it is clearly visible that prepregs are characterized by good fibres alignment and dense fibres bundles integrity. Moreover, kniting lines of fibres visible as black lines across reinforcement, as well as extensive resin on the surface is indicated as yellowish spots.

Figure 60: Typical structure of prepregs surface obtained by means of light microscope, with visible knitting, and extensive resin in the form of yellowish spots.

Figure 61: Images of fabricated plates by means of compression moulding using smaller (on the left) and larger pieces of tacky prepregs.

As it was mentioned in the methodology section, two different approaches were applied depending on type of the wastes and especially state of materials curing. In the first step, prepregs in tacky state were processed using parameters collected in table presented in methodology section. Prior to processing of prepregs, the waste materials were cut into two different size of pieces, marked as TS2/26 'larger' and TS3/26 'smaller'. In the result of first trials of the reprocessing process, flat composite panels with dimensions of 15 × 27 cm and a thickness of approximately 4 mm were successfully manufactured (Fig. 61). To evaluate the quality of the recycled composites, scanning electron microscopy (SEM) observations and mechanical testing were subsequently performed for evaluation of reprocessing effects. Below, in Table 13 they are collected measured mechanical values achieved in the results of tensile strength, bending and impact tests.

Sample name	Young's modulus [MPa]	Tensile strength [MPa]	Flexural modulus [MPa]	Flexural strength [MPa]	Charpy impact strength [kJ/m2]
TS2/26	5780	88,1	28000	261	44,95
TS3/26	6410	47,9	31700	221	38,23

Table 13: Parameters of composites plastes based vitrimer wastes after compression moulding reprocessing

Analyzing the obtained results it can be clearly seen that size of the compressed pieces significantly influence especially tensile strength values, thus smaller pieces size can be more suitable for further processing. SEM observations indicated good quality of obtained materials without visible porosity and dry fibers confirming satisfying infiltration quality.

In contrast to tacky materials, materials produced from previously reprocessed prepreg scraps in enduring state are more challenging to recycle, indicating further the need for optimization of processing parameters in subsequent reprocessing cycles. The incorporation of a limited amount of virgin vitrimer resin during reprocessing may improve material homogeneity and contribute to the production of more uniform composite structures.

5. KPI Assessment

This section, from table 14 to table 17, summarizes the performance of the demonstrated processes relative to the project Key Performance Indicators (KPIs). The assessment considers the experimental results obtained during the demonstrations and verifies the feasibility, functionality, and current maturity of the developed technologies. The status labels are to be interpreted as follows:
"Demonstrated" indicates that the KPI planned for the end of the project was reached during this demonstration already. "In progress" indicates that the KPI has not yet been reached, but is on track as can be expected at that stage of the project. "Open" indicates KPIs that could not be evaluated at this stage (e.g. those related to the final demonstrator parts).

TARGET KPI	STATUS
GLASS TRANSITION TEMPERATURE (T_G): ≥170 °C	Demonstrated
STORAGE CONDITIONS: STABLE AT 17-25 °C (ROOM TEMPERATURE)	Demonstrated
TAPES PROCESSABLE IN ENDURING STAGE	Demonstrated

Table 14: KPI assessment for the vitrimer material

KPI	Target	Status	Notes
Deposition Speed	1.2 m/s	**In progress**	1.2 m/s demonstrated with standard reference prepreg (April 2026); AFP placement with TOSCA vitrimer prepreg requires flash lamp heating to maintain high temperature at high speed.
Material Throughput	Max achievable - current configuration	In progress	AFP-X 4× 1/2" mechanically ready; FScanH scanning at 1.2 m/s demonstrated with TOSCA vitrimer prepreg. AFP placement at 1.2 m/s with TOSCA material pending flash lamp integration.
Inspection Speed Compatibility	In-line with AFP at 1.2 m/s	**Demonstrated**	FScanH operational at 1.2 m/s after hardware changes.
Spatial Resolution	~50 µm	Demonstrated	Sensor calibrated and operational at a spatial resolution of 34 µm

Table 15: KPI assessment for Lay-up inspection

KPI	Target	Status	Notes
Deposition Speed	1.2 m/s	In Progress	Adaptations to the equipment are required to increase temperature and pressure.
Panel production	Partner-defined panel number, dimensions, and configuration	**Demonstrated**	Panels were successfully produced according to the definitions and specifications provided by the partners.
Sensor layup	Demonstration of AFP lay-up using tapes with embedded sensors	**Demonstrated**	First trial of the lay-up of tapes with embedded sensors successfully demonstrated.

Table 16: KPI assessment for lay-up activities

Target KPI	Status	Partners involved
Damage Detection Accuracy (SHM): ≤10% position error	Demonstrated	Impact event location was successfully achieved when training with multiple energy levels. Additionally, energy quantification was achieved with error below 13%.
Simulation Accuracy (Delamination): ≤5% error	In progress	Delamination damage due to impact was successfully modelled, and the affected area trend predicted matched the experimental one. However, multiple experimental and numerical uncertainties (e.g. NDT accuracy, combined damage modes) precludes the achievement of the proposed KPI.
Manual Repair Time: - 50%	Open	For final demonstration only
Human Error Reduction (Repair): -60%	Open	For final demonstration only
Scrap Reduction (welding CF/CNT-tapes and CCF-filaments): - 15%	Open	For final demonstration only
Manufacturing Time Reduction (welding): - 25%	Open	For final demonstration only
Manufacturing Cost Reduction (welding): - 10%	Open	For final demonstration only

Table 17: KPI assessment related to SHM, joining / welding and repair

6. CONCLUSIONS

The work performed in this reporting period demonstrated the feasibility of processing and evaluating vitrimer-based thermoset composite materials across the main stages of the project workflow, from material formulation and tape production to automated manufacturing, curing, joining, repair, monitoring, digitalisation, and recycling. Overall, the results confirm the potential of the TS-1 vitrimer-based system for recyclable composite applications, while also identifying the main processing challenges that must be addressed in the next project phase.

The TS-1 vitrimer formulation and the corresponding prepreg tapes were successfully produced and characterised. The material showed stable storage behaviour in the enduring state at room temperature and achieved the required glass transition temperature after full cure. The tape production process was also demonstrated, although several improvements were identified, particularly regarding tape width tolerance, maximum roll length, release film configuration, and cutting quality. These aspects are important for improving the robustness of future AFP processing activities.

Automated lay-up of the vitrimer-based tapes was demonstrated using AFP equipment. At FIDAMC, the AFP-XS head was successfully adapted to process the 1/2-inch vitrimer tapes and produce representative panels according to partner requirements. However, the material required thermal activation and sufficient contact time to achieve stable adhesion, resulting in reduced deposition speeds compared with conventional tacky prepreg materials. Therefore, while panel production and the lay-up of prepreg tapes with previously embedded magnetoresistive sensors were successfully demonstrated, the 1.2 m/s deposition speed was not demonstrated for this material system with the AFP-XS configuration. In parallel, the integration of quality monitoring technologies was demonstrated using the AFP-X platform, where the FScanH system was validated at the target inspection speed and spatial resolution. Furthermore, the slight heating of the tape after unwinding is expected to significantly reduce its stiffness, thus facilitating the panel production process.

The curing and consolidation studies confirmed that the TS-1 vitrimer-based laminates can be fully cured using industrial processing routes. Both hot press and autoclave curing achieved high degrees of cure, above 97%, demonstrating the effectiveness of the defined thermal cycle. However, the final laminate quality was strongly influenced by the consolidation pressure. Hot-press-cured laminates showed a flatter and more uniform profile, higher DSC and DMA T_g values, and significantly improved ILSS performance compared with the autoclave-cured laminates. These results indicate that higher pressure improves laminate consolidation and interlaminar quality. In contrast, vacuum-only oven curing showed important limitations, mainly related to insufficient compaction pressure, persistent porosity, and incomplete ply consolidation.

The joining activities provided valuable information on the feasibility and limitations of welding vitrimer-based composite laminates. Induction welding, under the current equipment configuration, did not produce mechanically viable joints due to non-uniform heating and insufficient consolidation pressure. Resistance welding showed more promising results, with measurable joint performance and acceptable interfacial contact in some specimens. However, the variability observed in the mechanical results and the poor fracture toughness values indicate that further optimisation is required, especially regarding pressure application, thermal uniformity, and process repeatability. Furthermore, the addition of a surface film of TS-1 vitrimer on the surfaces to be welded is expected to facilitate the exchange of disulfide bonds and, therefore, the welding.

Repair activities demonstrated the practical implementation of repair concepts adapted to vitrimer-based composite materials. Initial self-healing repair trials without patch showed limited effectiveness, suggesting that the applied temperature and pressure were not sufficient to activate the repair mechanism. Patch repair processes were successfully implemented using vitrimer prepreg patches, with and without

additional vitrimer resin adhesive. Inspection and mechanical validation activities are ongoing, and further testing will be required to quantify the structural recovery and confirm the effectiveness of the repair process.

The integration and evaluation of structural health monitoring technologies were also demonstrated at coupon level. Magnetostrictive sensing showed the ability to detect impact-related changes, with results that correlated with ultrasonic inspection in commercial composite panels and partially in the vitrimer-based panels. In parallel, acoustic emission-based monitoring demonstrated promising impact localisation and energy estimation capabilities. These results support the feasibility of integrating monitoring technologies into composite structures manufactured with the developed materials, although further validation is required at larger scale and under more representative service conditions.

The digitalisation activities established a structured basis for data management and digital twin implementation. Manufacturing, inspection, process, simulation, and damage-related data were integrated into an HDF5-based data structure, supporting a continuous digital thread between material, manufacturing, monitoring, and simulation information. The development of database structures, graphical interfaces, and FEM-based damage prediction models provides an important foundation for future digital twin implementation at demonstrator level.

Finally, the recyclability of the vitrimer-based composite system was addressed through laboratory-scale recycling and compression moulding trials using vitrimer-based scraps. The work demonstrated the potential to reuse cured waste material within new composite components, although challenges remain regarding scrap geometry, viscosity during reprocessing, consolidation quality, and the possible need for additional resin. These results confirm the feasibility of the recycling approach at laboratory scale and provide a basis for further optimisation.

In conclusion, the project has successfully demonstrated the main processing and functional capabilities of the developed vitrimer-based thermoset composite system at material, coupon, and panel level. The results confirm the relevance of vitrimer chemistry for recyclable composite structures and show that the material can be processed, cured, monitored, repaired, joined, digitally represented, and recycled using adapted industrial approaches. At the same time, the work highlights that pressure, temperature control, tack activation, tape quality, and process repeatability are critical factors for achieving robust and scalable manufacturing. Future work should therefore focus on improving tape production quality, optimising AFP processability, increasing consolidation efficiency under industrial conditions, improving joining and repair robustness, and extending SHM, digital twin, and recycling validation towards larger and more representative demonstrators. This will not only require tuning of process parameters, but also the modification and extension of existing equipment (lay-up, welding, repair) to allow their operation at the required parameters (most notably temperature and pressure).

Although all these improvements and optimizations will be carried out on the material produced with the TS-1 vitrimer, its reformulation is also planned to broaden the current temperature window for activating its dynamism, which is very narrow due to the high Tg requirement. Different strategies will be explored that allow for both exchange and reorganization of disulfide bonds without causing their degradation. The study will be conducted at the resin level, and depending on the results obtained, a welding proof of concept at small scale could be considered in WP8 with panels manufactured in press or vacuum bag using manually produced prepreg.